Identifying atmospheric processes favouring the formation of physical features in the Mount Brown South ice core

By

Lingwei Zhang

Bachelor of Marine and Antarctic Science with Honours

University of Tasmania

Supervisors: Dr Tessa Vance, Dr Alexander Fraser, Dr Lenneke Jong

A thesis submitted in partial fulfilment of the requirements of the Bachelor of Marine and Antarctic Science with Honours at the Institute for Marine and Antarctic Studies (IMAS), University of Tasmania.

July 2020

Declaration

This thesis contains no material which has been accepted for the award of any other degree or diploma in any tertiary institution, and that, to the best of the candidate's knowledge and belief, the thesis contains no material previously published or written by another person, except where due reference is made in the text of the thesis.

Lingwei Zhang

10 July 2020

Abstract

The features preserved in ice cores provide crucial and unique records about the past atmospheric variability, offering the possibility to increase knowledge of the climate system and better predict future climate changes. Consequently, understanding the link between features in ice cores and the atmospheric processes causing them is key to interpreting the palaeoclimate information preserved in Antarctic ice. Ice cores from Mount Brown South (MBS), East Antarctica, were drilled to help understand the past atmospheric circulation variability in the southern Indian Ocean and southwest Pacific Ocean. In addition to chemical and isotopic records, high-resolution images of the ice core were made using an Intermediate Layer Ice Core Scanner (ILCS). Upon physical inspection of these images, there are visible bubble-free layers occurring frequently multiple times a year, and the origin of these features is still unknown. This project aims to determine whether the bubble-free layers in the MBS ice core can be related to atmospheric processes. Firn metamorphism refers to the change that occurs when firn transforms into water vapour and then deposits as ice at other ice grain surfaces. This results in an ice crust forming at the snow surface. The hypothesis of the research is that the ice crust driven by firn metamorphism is the precursor of the bubble free layers and that bubble free layers can be used as the proxy of atmospheric processes related to firn metamorphism. We use the newly available reanalysis products (ERA-5) from the European Centre for Medium range Weather Forecasts (ECMWF) to investigate the occurrence of firn metamorphism that may be related to atmospheric processes in the Mount Brown region including temperature inversions, wind scour, accumulation hiatuses and subsurface temperature gradients. We dated the ice cores using multiple annual chemical and isotopic horizons, and then used ERA-5 regional accumulation to estimate the month that the bubble-free layers occurred during 1979-2017. This information is used to detect the weather conditions occurring when the layers were formed in order to identify the most likely processes causing the bubble-free layers. The results show that accumulation hiatuses are the most likely atmospheric processes favouring the formation of bubble free layers in the Mount Brown South ice core.

Acknowledgements

I would like to express my deep gratitude to Dr Tessa Vance, Dr Alexander Fraser, Dr Lenneke Jong, my research supervisors, for their endless patient guidance, enthusiastic encouragement and help of this research work. I would also like to thank the wider IMAS/AAD ice core group for providing me the ice core data in this project. My grateful thanks are also extended to Camilla Crockart and Dr Andrew Klekociuk for their valuable and constructive suggestions of this research work.

I am also grateful to all my dear classmates and friends in University of Tasmania and Ocean University of China for their help, encourage, accompany and support throughout my honours year.

I am grateful to my parents and friends for their love, understanding and continuing support.

Table of Contents

Chapter 1 Literature Review

1. Antarctic ice core studies

The understanding of the climate system and the prediction of future climate change depends largely on knowledge of past atmospheric variability. However, past climate information is limited due to the short observational history and limited atmospheric data (King & Turner 1997; Souney et al. 2002; Tomczak 1994; Villalba et al. 1997). Because of the ability of preserving the records of past climate, ice core records play an increasingly crucial role in understanding the past atmospheric variability (Souney et al. 2002).

The mechanics of Antarctic glacial ice formation gives ice sheets the ability to record climate information (Cuffey & Paterson 2010). As snowflakes fall on the snow surface, they gradually lose their sharp edges of crystals and round off, which is caused by the great water pressure over sharp surface (the Kelvin equation). On the other hand, the temperature gradients generated by diurnal and seasonal variation result in evaporation and recondensation of snow (Legrand & Mayewski 1997). Both processes promote the transformation from snow to firn. In the firn zone, air is still able to move and exchange with atmospheric air. Afterward, with progressive compression and burial, the pore spaces get smaller and smaller with time and depth, until the pore channel closes off and bubbles form. With further burial and compression, firn becomes ice and the gas is permanently trapped in the ice. In addition to the air in bubbles, aerosols, impurities and ice properties can be trapped during snow formation or directly deposited on the snow surface (Bendel et al. 2013; Oeschger & Mintzer 1992). Finally, as the pressure increases with depth, bubbles gradually convert into air hydrates (Bendel et al. 2013).

Antarctic ice can reflect the climate at the time of snow deposition in both direct and indirect ways (Cuffey & Paterson 2010). A direct climate signal from ice cores is the gas preserved in bubbles, such as CO_2 or methane. The concentration of these gases in the ice itself is a direct measure of the gases in the atmosphere at the time of deposition. Another direct climate signal is the annual accumulation – the distance between the year horizons or annual layers are measured by chemical analysis of the ice (see section 1.2) and help calculate directly the amount of snow that fell and remained. Chemical composition and physical properties in ice

cores vary in response to climatic processes, which record the past climate indirectly. An example of an indirect climate signal is that of sea salt (sodium, Na^+ or chloride Cl^-). Sea salt is a proxy record of wind speed across the ocean surface, because there is a clear exponential relationship between wind speed and the lofting of sea salt aerosol into the atmosphere. When sea salt is measured in an ice core, an indirect measurement of wind speed is also made.

(1) Gases

Bubbles directly record atmospheric composition through preserving the past air. This has been confirmed by comparing the ice core measurements with atmospheric observation concentrations (Battle et al. 1996; Blunier et al. 1993; Etheridge, Pearman & Fraser 1992; Etheridge et al. 1996). Trapped gas has the same composition as the atmosphere at the time of ice formation (Schwander & Stauffer 1984). There is also a smoothing effect due to the time between snowfall at the surface and bubble close-off. This delay means that the air in the firn can still be exchanged with the atmosphere, so what is preserved in the ice core after bubble close-off is a smoothed record of atmospheric gasses. The degree of smoothing is often calculated by using the average accumulation and thus the time to bubble close-off, and can be confirmed using radioactive bomb pulse measurements.

The concentration histories of trace gases, such as CO_2, are significant for the investigation of the anthropogenic influence in climate change.

(2) Chemical composition

The chemical composition of ice cores varies for different reasons. Stable water isotopic ratios vary in proportion to temperature. The seasonal cycle of the ratio of oxygen isotopes (e.g. $\delta^{18}O$ and δDeuterium) have been widely used for ice core dating (Foster et al. 2006; Gragnani et al. 1998). The concentration of soluble impurities (nitrate, hydrogen peroxide) and hence the electrical conductivity of the ice can also vary annually. Hydrogen peroxide (H_2O_2) is one of the most concentrated impurities in snow and ice in polar region (Legrand & Mayewski 1997). The production of H_2O_2 is controlled by the intensity of sunlight. Because of the distinct seasonal sunlight difference, H_2O_2 concentration in summer snow is approximately more than five times higher than that in winter snow(Legrand & Mayewski 1997; Sigg & Neftel 2017). This character makes H_2O_2 particularly useful as a dating parameter(Morgan & van Ommen 1997). Usually, several indicators together promote the

accuracy of dating. Thus, the $\delta^{18}O$, H_2O_2 and electrical conductivity are used as palaeo-sunlight proxies to date the Mount Brown, Law Dome and Aurora basin ice core (Plummer et al. 2012; Smith & Ruddell 2001).

In addition, relatively accurate age scales can be determined by comparing the known time of volcanic eruptions and climate events with specific features. A change of winds can impact the dust concentration in ice. Volcanic eruptions provide impurities, leading to the formation of ash and acidic layers. Volcanic sulphate is also used to determine volcanic dating horizons in cores. Convective storm activity can make a significant difference to atmospheric nitrate production. All of those proxy measurements can be recorded and used to determine age scales and assess their accuracy.

(3) Physical properties

For physical properties of ice, some of them are sensitive to temperature change and climatic processes. The size and number of bubbles and other physical structures of ice are intimately related to different environmental process. For bubbles, due to the pressure increase, the overall trend of bubbles size and number density variation is to decrease with depth. During warm periods, smaller but more numerous bubbles form in ice cores (Lipenkov 2000). The size and number density of bubbles depends on the size of grains (the single crystal of ice). According to earlier studies (Lipenkov 2000; Spencer, Alley & Fitzpatrick 2006), environmental temperature and accumulation rate are the main influencing factors for the variation of grain size, and thus for the size and number density of bubbles in ice. The generation of large grain, or larger but fewer bubbles, often accompanies with high temperature and low accumulation rate. Bendel et al. (2013) suggest that impurity concentrations in ice should make a more significant difference on the density of bubbles and all of the three parameters are intimately related. Meanwhile, the number density of bubbles is proportional to the bubble size. They compared the distribution of cloudy bands (the layers with high impurity content) with high bubble number density layers and found a strong correlation between their locations.

2. Ice core dating

There are a lot of methods used to date ice cores. The first and most direct method is counting of annual layers. The layers are identified from measured variations in ice composition and impurity content. The most well-known method is analysing oxygen isotope ratio ($\delta\ ^{18}O$), which has been applied to numerous ice cores. The summer maxima in $\delta\ ^{18}O$ is taken to occur on the 1st of January of each year (Plummer et al. 2012; van Ommen & Morgan 1997). Like $\delta\ ^{18}O$ (the ratio of $H_2{}^{18}O$ to $H_2{}^{16}O$), the hydrogen isotope ratio (δD, the ratio of $HD^{16}O$ to $H_2{}^{16}O$) is exhibits summer maxima and is used for year boundary determination. Hydrogen peroxide (H_2O_2) is one of the the most concentrated impurities and clearest seasonal tracers in ice core studies, which also reaches a maximum in summer (Legrand & Mayewski 1997; Sigg & Neftel 2017). However, both of the two methods are limited to high accumulation sites due to the smoothing effect (Johnsen 1977; Neftel, Jacob & Klockow 1986). The sea salt species (Cl^-, Na^+, Ca^{2+} and Mg^{2+}) exhibit very strong seasonal cycle. In Antarctica, concentrations of sodium (Na^+), chloride (Cl^-) magnesium (Mg^{2+}) and calcium (Ca^{2+}) exhibit winter maxima because of more marine air mass advection over the ice sheet in winter. In summer, the input of HCl lead to a maximum of the ratio and hence the seasonality of Cl^- is weaker than Na^+. Acidic species (SO_4^{2-}, MSA(CH_3SO^{-3})) also exhibit summer maxima, which lead to the ratio of SO_4^{2-} /Cl^- and MSA are used as a summer marker(Legrand & Mayewski 1997). All of those chemical composition help determine annual layer in ice core, but the best dating is achieved when several seasonal signals are analysed and compared.

Another useful technique is using predetermined ages as markers, such as identifying volcanic eruptions events whose timing are recorded in documents. Acid and tephra from volcanic eruptions events are carried by the wind and distributed over vast areas. The volcanic ash layers can be detected and then used as reference horizons that can calibrate the age of the ice-core, as well as link different ice cores and records of past climate. High concentration of non-sea-salt sulphate ($nssSO_4^{2-}$) are used as the signal of volcanic eruptions (Plummer et al. 2012).

3. Climate reanalysis data

Climate reanalyses can be used to understand the link between physical features in ice cores and the atmospheric processes producing them. ERA-5 is the latest high-resolution atmospheric reanalysis products, providing a numerical description of the climate from 1950 to present (Gossart et al. 2019; Hersbach & Dee 2016; Urraca et al. 2018).

In this project, the following parameters will be analysed to determine any atmospheric processes that may happen and cause features in the Mount Brown South ice core.

Snowfall

ERA-5 snowfall data is the total snow that has fallen to the Earth's surface. It consists of snow due to the large-scale atmospheric flow (horizontal scales greater than around a few hundred metres) and convection where smaller scale areas (around 5km to a few hundred kilometres) of warm air rise. The snowfall record will show when snow has fallen at MBS, and then help determine sub-annual ice core dating which can give roughly where within a given year the features in ice core are occurring.

2 metre temperature

ERA-5 2 metre temperature is the air temperature at 2 m above the Earth's surface. It is calculated by interpolating between the lowest model level and the Earth's surface, taking account of the atmospheric conditions.

Skin temperature

ERA-5 skin temperature is the temperature at the Earth’s surface. The skin temperature is the theoretical temperature required to satisfy the surface energy balance. The temperature it represented is the uppermost surface layer temperature that can respond instantaneously to change of surface flux.

Atmospheric temperature inversions are generally calculated from radiosonde (weather balloon) profiles, but can also be detected by comparing 2 metre temperature with skin temperature (Fisher et al. 1983; Mayfield & Fochesatto 2013). When surface temperature inversion occurs, the 2 metre temperature should be warmer than the skin temperature. Thus,

the two temperatures will be used to explore if any temp inversions occur, the size and degree of the temperature inversion and if these coincide with any layers.

10 metre U and V wind component

The U (eastward) and V (northward) wind components at an altitude of 10 m above the ground are produced in all atmospheric reanalysis products.

The speed and direction of the horizontal 10 metre wind can be calculated from the U and V components. Near-surface wind will also be related to surface pressure and snowfall. It will change in speed and direction with storms, and it will also change if there is katabatic wind activity. These may both be related to the bubble free layers in the Mount Brown South ice core.

4. Firn metamorphism

"Firn" is an intermediate state between snow and ice. Firn metamorphism is driven by temperature gradients (Albert et al. 2004; Bingham 2011; Colbeck 1980; Davis, Arons & Albert 1996; Spencer, Alley & Fitzpatrick 2006). The rate of firn metamorphism is related to surface temperature and high local snowfall accumulation rate (Bingham 2011; Spencer, Alley & Fitzpatrick 2006). Large temperature gradient, high local snowfall accumulation rate and warm surface temperature can enhance firn metamorphism.

Firn metamorphism can be enhanced by large subsurface temperature gradient. Because larger temperature gradient can enhance the vapour transport facilitates the metamorphosis of the near-surface firm layers. In polar region, the temperature of snow in different depth is dominated by different processes. In the top 20-30 cm, temperature is controlled by diurnal changes of air temperature (Colbeck 1980; Courville et al. 2007). In the top 30-70 cm, weekly to seasonal variations in air temperature is the main influencing factor of snow temperature (Courville et al. 2007). At approximately 10 m depth below snow surface, the temperature remains constant, which is approximately the average annual air temperature (Courville et al. 2007). Thus, the temperature at the upper few centimetres of snow is dominated by the diurnal changes of air temperature. Consequently, the magnitude of the temperature gradient is also controlled by diurnal air temperature changes, except winter. In polar winter, there is no sun light. Snow is warmed from the deep ice and ground which

release the heat accumulated during the warmer months. Meanwhile, the cooler air in winter month cools the temperature of surface snow. With colder surface and warmer inside, a subsurface temperature gradient is established across the snowpack.

Firn metamorphism can be enhanced by warner air temperature. Because warmer air can hold more water vapour than air that is colder, the higher mean temperatures in summer, autumn and spring would allow more near-surface vapour exchange (Albert et al. 2004; Colbeck 1980).

Firn metamorphism can be enhanced by high snowfall accumulation rate (Spencer, Alley & Fitzpatrick 2006). Overburden pressure from snowfall produces a vertical stress field that increases with depth. This induces strain that leads to densification. High accumulation rate increases the amount of overburden pressure, resulting in enhancing firn metamorphism. The Mount Brown South ice core site is a high accumulation region where the rate of firn metamorphism could be high.

Besides, firn metamorphism can be further enhanced by wind-driven interstitial air movement due to ventilation (Albert 2002). Ventilation is the process by which atmospheric pressure changes cause interstitial air movement in firn and snow. The Mount Brown South ice core site is region experiencing constant katabatic winds, which can enhance the firn metamorphism.

According to previous studies, air temperature inversion, wind scour and accumulation hiatus are the atmospheric processes that could be important to firn metamorphism (Courville et al. 2007; Fegyveresi et al. 2018; Fisher et al. 1983).

Firn metamorphism during accumulation hiatus

Firn metamorphism can be enhanced during accumulation hiatus. Accumulation hiatus is lack of snowfall in several days with no cloud sky. As the snow deposit at surface being blown away by wind, without new snowfall, the firn layer is exposed under the force of solar radiation and diurnal air temperature change.

During daytime, through clear sky, intense sunshine brings downward short-wave radiation, generating a temperature maximum in the snow just below the surface (Alley & Koci 1990; Brandt & Warren 1993). At this time, the surface temperature is colder than the temperature

at the upper few centimetres of snow. The higher the temperature below the surface, the higher vapor-density gradients and vapor diffusivity will be.

During night-time, there is no solar radiation flux. Meanwhile, under calm and clear weather, surface temperature decreased rapidly due to upward longwave radiation. This effect hence cooling of snow surface at dark cold night. However, thermal conductivity of snow is small, the internal snow remained warm. Therefore, high temperature gradient persisted in the upper snow during the night. The upper surface is colder than snow beneath, driving vapour upward mass flux (Fegyveresi et al. 2018). Snow sublimed from the deeper warm region, diffuses across the pore and deposit on the cold snow above, forming and strengthening crusts. The process is enhanced at warm temperature and high temperature gradients (Adams & Brown 1983). Finally, some crusts buried by snowfall and preserved in ice.

In spring, summer and autumn, the relatively warm air temperature allows more near-surface vapour exchange. Cool dark night drives the formation of high temperature gradients below snow surface. During warm season, such as summer and early Autumn, more accumulation hiatus happened, enhancing the firn metamorphism.

In winter, although more and stronger temperature gradients occur, without warm temperature and enough water vapour, the formation of ice crusts at snow surface become harder.

Firn metamorphism during temperature inversion

A temperature inversion is a phenomenon that the air temperature increases with the increase in altitude. The same as accumulation hiatus, the clear sky during temperature inversion can enhance the firn metamorphism (Fegyveresi et al. 2018).

Firn metamorphism during wind scour

Wind scour occurs where strong katabatic winds persistently polish at the ice surface (Fisher 1983). The winds can completely remove the annual snowfall over the scour zones, increased absorption of short-wave solar radiation and enhanced vapour transport (Das et al. 2013). This process can enhance firn metamorphism, producing a wind-packed layer.

References

Adams, EE & Brown, RL 1983, 'Metamorphism of Dry Snow as a Result of Temperature Gradient and Vapor Density Differences', *Annals of Glaciology*, vol. 4, pp. 3-9.

Albert, M 2002, 'Effects of snow and firn ventilation on sublimation rates', *Annals of Glaciology*, vol. 35, pp. 52-56.

Albert, M, Shuman, C, Courville, Z, Bauer, R, Fahnestock, M & Scambos, T 2004, 'Extreme firn metamorphism: impact of decades of vapor transport on near-surface firn at a low-accumulation glazed site on the East Antarctic plateau', *Annals of Glaciology*, vol. 39, pp. 73-78.

Alley, RB & Koci, BR 1990, 'Recent Warming in Central Greenland?', *Annals of Glaciology*, vol. 14, pp. 6-8.

Battle, M, Bender, M, Sowers, T, Tans, PP, Butler, JH, Elkins, JW, Ellis, JT, Conway, T, Zhang, N, Lang, P & Clarket, AD 1996, 'Atmospheric gas concentrations over the past century measured in air from firn at the South Pole', *Nature*, vol. 383, no. 6597, pp. 231-235.

Bendel, V, Ueltzhöffer, KJ, Freitag, J, Kipfstuhl, S, Kuhs, WF, Garbe, CS & Faria, SH 2013, 'High-resolution variations in size, number and arrangement of air bubbles in the EPICA DML (Antarctica) ice core', *Journal of Glaciology*, vol. 59, no. 217, pp. 972-980.

Bingham, RG 2011, 'Book Review: The Encyclopedia of Snow, Ice and Glaciers', *Journal of Glaciology*, vol. 57, pp. 1171-1172.

Blunier, T, Chappellaz, JA, Schwander, J, Barnola, J-M, Desperts, T, Stauffer, B & Raynaud, D 1993, 'Atmospheric methane, record from a Greenland Ice Core over the last 1000 year', *Geophysical Research Letters*, vol. 20, no. 20, pp. 2219-2222.

Brandt, RE & Warren, SG 1993, 'Solar-heating rates and temperature profiles in Antarctic snow and ice', *Journal of Glaciology*, vol. 39, no. 131, pp. 99-110.

Colbeck, S 1980, 'Thermodynamics of snow metamorphism due to variations in curvature', *Journal of Glaciology*, vol. 26, pp. 291-301.

Courville, ZR, Albert, MR, Fahnestock, MA, Cathles IV, LM & Shuman, CA 2007, 'Impacts of an accumulation hiatus on the physical properties of firn at a low-accumulation polar site', *Journal of Geophysical Research: Earth Surface*, vol. 112, no. F2.

Cuffey, K & Paterson, WSB 2010, *The Physics of Glaciers 4th Edition*, Academic Press.

Das, I, Bell, R, Scambos, T, Wolovick, M, Creyts, T, Studinger, M, Frearson, N, Nicolas, J, Lenaerts, J & Van den Broeke, M 2013, 'Influence of persistent wind scour on the surface mass balance of Antarctica', *Nature Geosci*, vol. 6, pp. 367-371.

Davis, RE, Arons, EM & Albert, MR 1996, 'Metamorphism of Polar Firn: Significance of Microstructure in Energy, Mass and Chemical Species Transfer', in EW Wolff & RC Bales (eds), *Chemical Exchange Between the Atmosphere and Polar Snow*, Berlin, Heidelberg, pp. 379-401.

Etheridge, DM, Pearman, GI & Fraser, PJ 1992, 'Changes in tropospheric methane between 1841 and 1978 from a high accumulation-rate Antarctic ice core', *Tellus B*, vol. 44, no. 4, pp. 282-294.

Etheridge, DM, Steele, LP, Langenfelds, RL, Francey, RJ, Barnola, J-M & Morgan, VI 1996, 'Natural and anthropogenic changes in atmospheric CO2 over the last 1000 years from air in Antarctic ice and firn', *Journal of Geophysical Research: Atmospheres*, vol. 101, no. D2, pp. 4115-4128.

Fegyveresi, JM, Alley, RB, Muto, A, Orsi, AJ & Spencer, MK 2018, 'Surface formation, preservation, and history of low-porosity crusts at the WAIS Divide site, West Antarctica', *The Cryosphere*, vol. 12, no. 1, pp. 325-341.

Fisher, DA, Koerner, RM, Paterson, WSB, Dansgaard, W, Gundestrup, N & Reeh, N 1983, 'Effect of wind scouring on climatic records from ice-core oxygen-isotope profiles', *Nature*, vol. 301, no. 5897, pp. 205-209.

Foster, AFM, Curran, MAJ, Smith, BT, Van Ommen, TD & Morgan, VI 2006, 'Covariation of Sea ice and methanesulphonic acid in Wilhelm II Land, East Antarctica', *Annals of Glaciology*, vol. 44, pp. 429-432.

Gossart, A, Helsen, S, Lenaerts, JTM, Broucke, SV, Lipzig, NPMv & Souverijns, N 2019, 'An Evaluation of Surface Climatology in State-of-the-Art Reanalyses over the Antarctic Ice Sheet', *Journal of Climate*, vol. 32, no. 20, pp. 6899-6915.

Gragnani, R, Smiraglia, C, Stenni, B & Torcini, S 1998, 'Chemical and isotopic profiles from snow pits and shallow firn cores on Campbell Glacier, northern Victoria Land, Antarctica', *Annals of Glaciology*, vol. 27, pp. 679-684.

Hersbach, H & Dee, D 2016, *ECMWF*, viewed 29 July 2019, <https://www.ecmwf.int/en/newsletter/147/news/era5-reanalysis-production>.

Johnsen, SJ 1977, 'Stable isotope homogenization of polar firn and ice. ', *Isotopes and impurities in snow and ice*, vol. 118, pp. 210-219.

King, JC & Turner, J 1997, *Antarctic Meteorology and Climatology*, Cambridge Atmospheric and Space Science Series, Cambridge University Press, Cambridge.

Legrand, M & Mayewski, P 1997, 'Glaciochemistry of polar ice cores: A review', *Reviews of Geophysics*, vol. 35, no. 3, pp. 219-243.

Lipenkov, VY 2000, 'Air bubbles and air-hydrate crystals in the Vostok ice core', paper presented to Physics of Ice Core Records, 2000.

Mayfield, JA & Fochesatto, GJ 2013, 'The Layered Structure of the Winter Atmospheric Boundary Layer in the Interior of Alaska', *Journal of Applied Meteorology and Climatology*, vol. 52, no. 4, pp. 953-973.

Morgan, V & van Ommen, TD 1997, 'Seasonality in late-Holocene climate from ice-core records', *The Holocene*, vol. 7, no. 3, pp. 351-354.

Neftel, A, Jacob, P & Klockow, D 1986, 'Long-term record of H2O2 in polar ice cores', *Tellus B*, vol. 38B, no. 3-4, pp. 262-270.

Oeschger, H & Mintzer, IM 1992, 'Lessons from the Ice Cores: Rapid Climate Changes During the Last 160,000 Years', in IM Mintzer (ed.), *Confronting Climate Change: Risks, Implications and Responses*, Cambridge University Press, Cambridge, pp. 55-64, via Cambridge Core (Cambridge University Press).

Plummer, C, Curran, M, Van Ommen, T, Rasmussen, S, Moy, A, Vance, T, Clausen, H, Vinther, B & Mayewski, P 2012, 'An independently dated 2000-yr volcanic record from Law Dome, East Antarctica, including a new perspective on the dating of the 1450s CE eruption of Kuwae, Vanuatu', *Climate of the Past*, vol. 8, pp. 1929-1940.

Schwander, J & Stauffer, B 1984, 'Age difference between polar ice and the air trapped in its bubbles', *Nature*, vol. 311, no. 5981, pp. 45-47.

Sigg, A & Neftel, A 2017, 'Seasonal Variations in Hydrogen Peroxide in Polar Ice Cores', *Annals of Glaciology*, vol. 10, pp. 157-162.

Smith, BT & Ruddell, A 2001, *Snow accumulation in Wilhelm II Land, East Antarctica. Antarct.*, vol. 22, 22 vols., Research report (Antarctic CRC).

Souney, JM, Mayewski, PA, Goodwin, ID, Meeker, LD, Morgan, V, Curran, MAJ, van Ommen, TD & Palmer, AS 2002, 'A 700-year record of atmospheric circulation developed from the Law Dome ice core, East Antarctica', *Journal of Geophysical Research: Atmospheres*, vol. 107, no. D22, pp. 1-9.

Spencer, MK, Alley, RB & Fitzpatrick, JJ 2006, 'Developing a bubble number-density paleoclimatic indicator for glacier ice', *Journal of Glaciology*, vol. 52, no. 178, pp. 358-364.

Tomczak, M 1994, *Regional oceanography : an introduction*, Pergamon, Oxford, England ; New York.

Urraca, R, Huld, T, Gracia-Amillo, A, Martinez-de-Pison, FJ, Kaspar, F & Sanz-Garcia, A 2018, 'Evaluation of global horizontal irradiance estimates from ERA5 and COSMO-REA6 reanalyses using ground and satellite-based data', *Solar Energy*, vol. 164, pp. 339-354.

van Ommen, TD & Morgan, V 1997, 'Calibrating the ice core paleothermometer using seasonality', *Journal of Geophysical Research: Atmospheres*, vol. 102, no. D8, pp. 9351-9357.

Villalba, R, Cook, ER, D'Arrigo, RD, Jacoby, GC, Jones, PD, Salinger, MJ & Palmer, J 1997, 'Sea-level pressure variability around Antarctica since A.D. 1750 inferred from subantarctic tree-ring records', *Climate Dynamics*, vol. 13, no. 6, pp. 375-390.

Chapter 2: Manuscript

Abstract

The features preserved in ice cores provide crucial and unique records about the past atmospheric variability, offering the possibility to increase knowledge of the climate system and better predict future climate changes. Consequently, understanding the link between features in ice cores and the atmospheric processes causing them is key to interpreting the paleoclimate information preserved in Antarctic ice. Ice cores from Mount Brown South (MBS), East Antarctica, were drilled to help understand the past atmospheric circulation variability in the southern Indian Ocean and southwest Pacific Ocean. In addition to chemical and isotopic records, high-resolution images of the ice core were made using an Intermediate Layer Ice Core Scanner (ILCS). Upon physical inspection of these images, there are visible bubble-free layers occurring frequently multiple times a year, and the origin of these features is still unknown. This project aims to determine whether the bubble-free layers in the MBS ice core can be related to atmospheric processes. Firn metamorphism refer to the change of firn that transform into water vapour and then deposit as ice at other grain surface, which result in ice crust form at snow surface. The hypothesis of the research is that the ice crust driven by firn metamorphism is the precursors of the bubble free layers and the bubble free layer can be used as the proxy of atmospheric processes related to firn metamorphism. Then, we use the newly available reanalysis products (ERA-5) from the European Centre for Medium range Weather Forecasts (ECMWF) to investigate the occurrence of firn metamorphism related atmospheric processes in the Mount Brown region including temperature inversions, wind scour, accumulation hiatuses and subsurface temperature gradient. We dated the ice cores using multiple annual chemical and isotopic horizons, and then used ERA-5 regional accumulation to estimate the month that the bubble-free layers occurred during 1979-2017. This information is used to detect the weather conditions occurring when the layers were formed in order to identify the most likely processes causing the bubble-free layers. The result shows that accumulation hiatus is the atmospheric processes favouring the formation of physical features (bubble free layer) in the Mount Brown South ice core.

Introduction

In Antarctica, near-surface snow physical properties (e.g., stratigraphy, density) are altered by weather-related processes such as strong winds and temperature fluctuations, producing features at the snow surface and preserving them in the deeper ice. Those features preserved in ice cores provide crucial and unique records about the past atmospheric variability, offering the possibility to increase the knowledge of the climate system and better predict the future climate changes (Porter & Mosley-Thompson 2014; Vance et al. 2016). Consequently, interpretation of these physical features may be complementary to the traditional chemical interpretation of ice cores, which help understand important aspects of past climate (Jouzel 2001).

Considering the lack of information on the past climate conditions formed in the Indian Ocean and southwest Pacific Ocean, four ice cores from a new site in coastal East Antarctica named Mount Brown South (MBS) were drilled in 2017/18 and will be used to help understand long-term climate variability in the southern Indian Ocean and southwest Pacific Ocean (Masson-Delmotte et al. 2003; Vance et al. 2016). The 295-metre-long MBS main core, which is the longest of the four MBS ice core, is expected to span the last millennium (see section 2 for site details).

Upon physical inspection of the core, bubble-free layers at sub-annual resolution, about 1–2 mm thick, were noticed (Fig. 1). Similar bubble-free layers have been documented in other ice cores (Bendel et al. 2013; Fegyveresi et al. 2018; Fitzpatrick et al. 2014; Orsi et al. 2015). The origin of these features in the MBS ice core has yet to be studied. A number of other studies have suggested that the bubble free layers in other ice cores could be related to atmospheric processes and could be used as a paleoclimatic indicator.

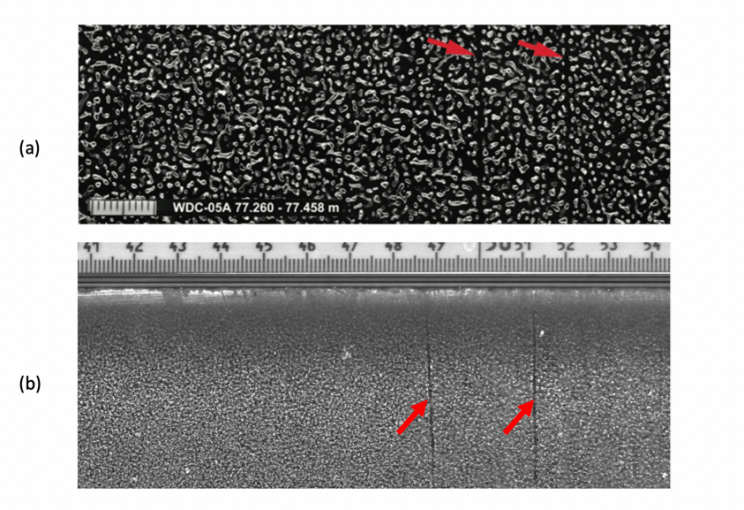

Figure 1 (a) Bubble free layers in WAIS Divide ice core (Orsi et al. 2015). They are about 1mm thick and can only be detected in the upper 600m of the ice. (b) Similar bubble free layers in MBS ice core, about 1–2 mm thick

There are three main kinds of bubble-free layers investigated in previous studies.

Bendel and others (2013) observed some bubble-free cloudy bands only appearing below certain depth (below ~700 m depth) where the bubbles start to convert to air hydrates. The presence of a high concentration impurities in the ice core promotes the bubble-to-hydrate transformation process, which leads to the formation of bubble-free layers. However, the MBS ice core is only 300 m long, so it isn't deep enough for bubble-to-hydrate transformation process and thus we don't expect its bubble free layers to be a result of some of the deep ice processes.

Melt layers also present as bubble-free layers in other studies, which only irregularly appear in ice layers, and generally form in summer. Compared with the bubble-free layers in the MBS ice core, the melt layers are often thicker (typically 1–100 mm in thickness), and have ragged edges, particularly in shallow cores, and only appear in summer. The MBS ice cores were drilled from the dry-snow zone above the 2000 m contour (Trusel, Frey & Das 2012). Summer melt is likely to be totally absent in this region.

Orsi et al. (2015) observed numerous bubble-free layers in the WAIS Divide ice core which are similar in appearance and depth to the bubble-free layers in the MBS ice core (Fig. 1). In order to detect melt events, they analysed the Kr/Ar and Xe/Ar ratios of those layers. Kr and Xe are highly soluble in liquid water, and both are more soluble than Ar. If the bubble-free

layer contains melted and refrozen ice, the Kr/Ar and Xe/Ar ratios should be higher than ice that has not melted. However, the result indicated that no sufficient melt was detected in those bubble-free layers. Thus, there is a strong evidence to suggest that the bubble-free layers in the MBS ice core may be generated by processes other than melt events.

The origin of this third kind of bubble free layer is thought to be via firn metamorphism. These bubble-free layers are thin, can occur in any season and typically can be observed in low accumulation regions experiencing constant katabatic winds. Fujii and Kusunoki (1982) measured the sublimation and condensation at the ice sheet surface and suggested that the bubble-free layers may be generated by the condensation of water vapour. By this mechanism, solar radiation warms a layer of subsurface snow, leading to a temperature gradient (i.e., upper snow is colder than subsurface snow) and subsequent upward transport of water vapour. As the surface temperature changes due to diurnal temperature variation,water vapour condenses and fills the vacant places of snow crystal, forming ice crust. Further, Albert and others (2004) argue that the persistent and strong katabatic wind action on the East Antarctic plateau enhances the formation of bubble-free layers by increasing enhanced vapour transport and air ventilation in firn. The near-surface firn is exposed to subsurface temperature gradients, driving vapour transport through diffusion. Besides, due to the natural convection driven by buoyancy and ventilation driven by wind, the interstitial air movement also drives vapor transport, and then enhance firn metamorphism. During the summer from 2008 to 2013, Fegyveresi and others (2018) measured wind, humidity, temperature and insolation at the WAIS Divide site and suggested that the frequency and thickness of bubble-free layers probably could be used as a proxy for the occurrence of temperature inversions which can enhance the firn metamorphism (Fegyveresi et al. 2018; Fitzpatrick et al. 2014).

In summary, there are main three processes producing bubble-free layers in ice cores. First of all, below a certain depth (~ 700 m), in response to the change of overburden pressure, the bubbles in ice decrease, shrink and finally become invisible, forming bubble-free cloudy bands (Bendel et al. 2013; Cuffey & Paterson 2010; Shoji & Langway 1982). The second kind of bubble free layer is the melt layer generated by glacier snow melting and refreezing. The third kind of bubble free layer is crusts formed by firn metamorphism. As mentioned before, bubble-free cloudy bands and melt layers are very unlikely to be the origin of the bubble free layers observed in MBS ice core. Thus, firm metamorphism and related

atmospheric processes and their relationship with bubble free layer formation are analysed in this study.

There are multiple mechanisms that may induce firn metamorphism. First of all, the subsurface temperature gradients caused by diurnal temperature changes can cause near-surface vapour diffusion in polar snow and firn, which induces vapour-driven redeposition and crystal growth in the top of firn, forming thin ice crusts over only hours or days. The temperature gradient driven by seasonal temperature change needs years to form crusts (Albert et al. 2004). Then, vapour transport can be further enhanced by wind-driven interstitial air movement due to ventilation, especially in high-permeability firn (Albert 2002; Albert et al. 2004). Thus, weather favouring temperature gradients and air movement at the snow surface are the main processes investigated in this study. According to previous studies, air temperature inversion, wind scour and accumulation hiatus are the atmospheric processes that could be important to firn metamorphism (Courville et al. 2007; Fegyveresi et al. 2018; Fisher et al. 1983). In addition, the temperature gradient at the snow surface generated by daily temperature change is also analysed in here.

This paper focuses on the records extracted from three short cores collected from the MBS coring site, East Antarctica, spanning the satellite era (1979-2017). It explores links between atmospheric processes and bubble-free layers in ice cores by comparing the estimated month of bubble-free layer formation with the time when those atmospheric processes happened.

Datasets

1. Ice core site details and analysis

The Mount Brown South ice core site is located about 380 km east of Davis station and at an elevation of 2084 m on the East Antarctic Plateau (Fig. 1). The site is characterised by a high annual accumulation (> 200 mm year^{-1}), a dry snow zone (Oza et al. 2011; Trusel, Frey & Das 2012) with persistent katabatic winds resulting in aligned snow structure indicating the presence of developed sastrugi (Fraser, Young & Adams 2014). Summer melt is very unlikely at the Mount Brown South site (Vance et al. 2016).

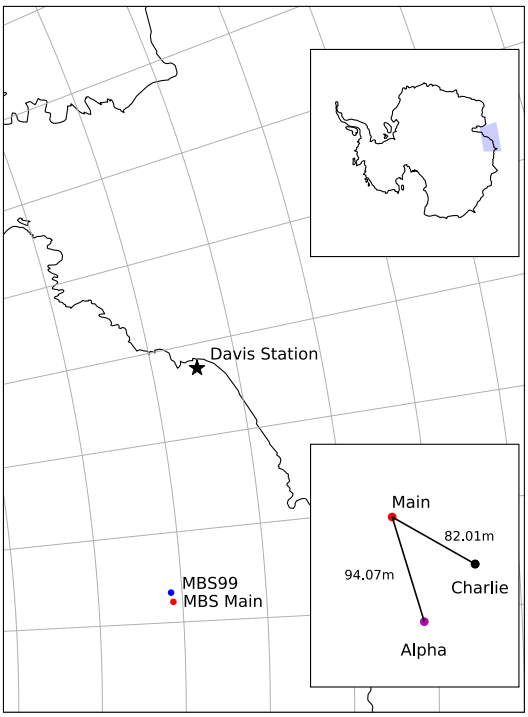

Figure 2. The location of Mount Brown and 3 ice cores and the distance between each core. The MBS99 ice core was drilled at an altitude of 2078 m in 1999. The location of cores: Main core (86.312417E, 69.110900S); Alpha core (86.314725E, 69.110704S); Charlie core (86.31355E, 69.110283S); MBS99 (85.9985E, 69.1310S). The distance between MBS99 and Main core is about 12.64 km.

The three MBS ice cores presented in this paper were drilled at an altitude of 2,084m during the austral summer of 2017-2018. Main core was drilled to 295 metres using a Hans Tausen drill. The Alpha and Charlie core, two short 20-25 m cores spanning the satellite era, were drilled using the Kovacs system. All three cores are physically separated at the site by a minimum of 50 metres. The Alpha core is situated 94.07 m to the east of the Main core. The

Charlie core is situated 66.04 m to the north of the Alpha core, which places it around 82.01 m to the northeast of Main.

1.1 Trace chemistry and water stable isotope records

Three separate ice cores from the MBS site were used in this study. The isotopic and chemical data of three ice cores are measured individually, providing us the accumulation information of three different locations in one site.

Isotopic and chemical data from the upper 20 m (snow depth) of the three MBS ice core is used for establishing high-resolution annual dating of the MBS ice core over the recent 40 years. This help determine the annual accumulation for three individual core and average site accumulation. Meanwhile, the establishment of year boundaries in three cores help us determine the month when the bubble-free layers in three different ice cores formed.

The MBS ice core chemical record contained seasonal cycles, which were used to date the firn core. Seasonal cycles in isotopic and trace chemical records have been successfully used to date high resolution ice cores elsewhere in Antarctica (Foster et al. 2006; Legrand & Delmas 1985; Minikin et al. 1994; van Ommen & Morgan 1997; Welch, Mayewski & Whitlow 1993). The annual cycles in water isotopes ($\delta^{18}O$ and δDeuterium) and the major ion species methanesulfonic acid (MSA, CH_3SO^{-3}), chloride (Cl^{-}), sodium (Na^{+}), magnesium ($Mg2^{+}$), calcium (Ca^{2+}) and SO^4/Cl, which provided the clearest cyclicity of all of the chemical components and were used for dating.

Stable water isotope (δ ^{18}O and δ Deuterium) analysis were performed on a Picarro L2130-*i* isotopic water analyser. Aliquots of water were sampled by a Picarro liquid auto-sampler and injected into a Picarro high precision vaporization module (A0211) and held at temperature of 110°C with the vapour sent to the Picarro L2130-*i* isotopic water analyser. Isotopic values are expressed as per mil (‰) and relative to the Vienna Standard Mean Oceanic Water (V-SMOW) standard. The standard deviation (SD) of the δ ^{18}O values for repeated measurements of laboratory reference water samples was less than 0.05 ‰ and less than 0.5 ‰ for δ Deuterium.

Trace chemical species were analysed according to the methods described in Palmer et al., (2001). Briefly, trace clean samples at 3 cm resolution were analysed via trace ion

chromatography under clean conditions. The ice cores were analysed for a range of ions using suppressed ion chromatography techniques (Legrand, Angelis & Maupetit 1993) and Dionex equipment. Nitrate and other anions were preconcentrated from a 6 mL sample using a 4 mm TAC-LP1 concentrator column and determined on a DX500 ion chromatograph with a 2 mm Ionpac AS14 column. Nitrate eluted at 12 minutes using a gradient method with a sodium tetraborate eluent.

1.2 Ice core scan

The physical features of three MBS ice cores have been imaged by Intermediate Layer ice Core Scanner (ILCS). The line scanner produces high-quality images, recording the bubble free layers and their depth.

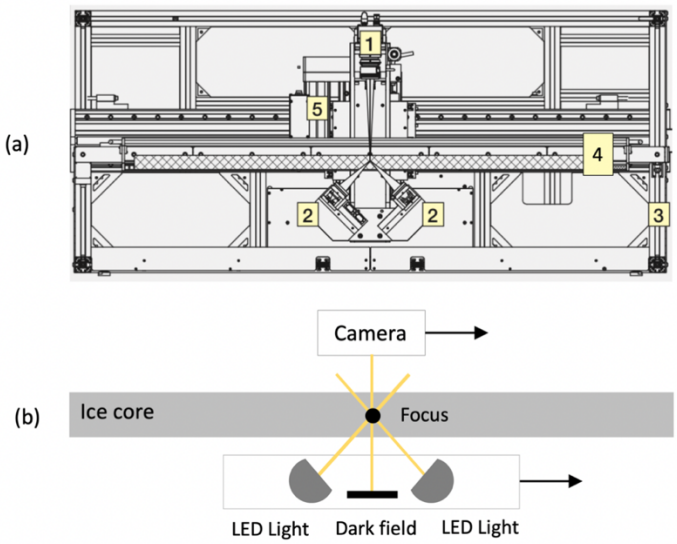

Figure 3. (a) System components of the Intermediate Layer Core Scanner. 1 Detector with line scan camera; 2 Transmitted light; 3 Base frames; 4 Ice core carrier; 5 Translation stage, z-axis, (b) Ice core scan process. Image courtesy of ILCS Operating manual, Schäfter & Kirchhoff, Germany.

The ILCS is designed to perform a transect of a planar ice core at a predetermined depth, providing an intermediate layer scan of the ice core for subsequent image analysis. Typically, the ice sample is cut as an ice slab, which is about 1m long, 100mm wide and 40mm thick. Before imaging, ice cores have been cut lengthwise. The ice core surfaces were planed using a mechanical thicknesser, with additional polishing by hand using a stainless steel microtome blade if necessary. Nearly half of the ice core was used to analyse various visual stratigraphy

(Fig. 4). Their upper and lower surfaces were microtome polished. Then, ice sample was put in the ice core carrier and pushed by hand into the scanner base frame.

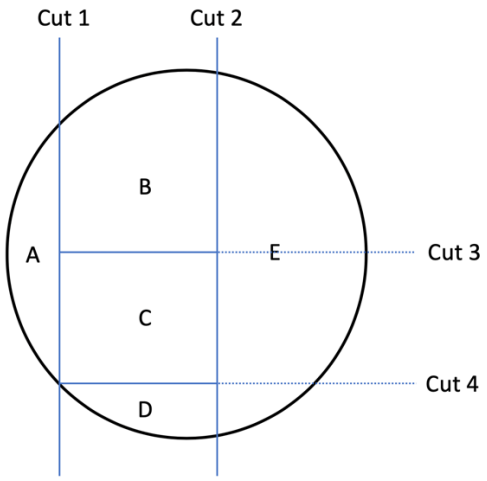

Figure 4. Sample ice core sectioning strategy. A: Archive; B: a suite of other chemicals using a Continuous Flow Analysis (CFA) system; C: trace chemistry from discrete samples; D: water stable isotopes analysis; E: The E section is actually scanned in this research. A small section is cut off the rounded edge to make a slab with two parallel flat surfaces, and then the larger flat surface is scanned after planing and microtoming it to a smooth finish.

Ice samples were photographed by a computer-controlled line scan camera at a resolution of 2048-pixels. The transmitted light under the ice sample moved synchronously with a camera above the ice, along the core axis (Fig. 3). As the light is focused in the ice slab at a 45° angle relative to the ice surface, the line scan camera can not capture light until impurities or bubbles scatter light into the camera. Because the light passes through the transparent ice, clear ice is recorded as dark areas in the ice core scan image. As the concentration of inclusions in ice samples increases, the brightness in the scanned image also increases. Consequently, regions with bubbles and impurities appear light while the bubble-free layers were recorded as thin dark lines aligned perpendicular to the longitudinal axis of the core.

2. Reanalysis data set

To analyse atmospheric processes, we need long-term meteorological records at the ice core sites. However, the lack of surface meteorological observations is an impediment to analysing the climate variability at the MBS ice core site. One common method of overcoming the difficulties arising from the inadequate observational network is to use

gridded atmospheric data at high temporal resolution (i.e., reanalysis data) to represent key atmospheric parameters. In recent years, atmospheric reanalysis data have been widely used for various studies such as surface climate characteristics of the Antarctic region as well as large-scale atmospheric forcing mechanisms modifying the surface climate variables (Costi et al. 2018; Hines, Bromwich & Marshall 2000; Lenaerts et al. 2012; Maksym & Markus 2008). There are two widely-used, recent reanalysis products from the European Centre for Medium-Range Weather Forecasts (ECMWF), ERA-5 and ERA-Interim, which can provide a numerical description of the key climate variables from 1979 to present (Gossart et al. 2019; Hersbach & Dee 2016; Urraca et al. 2018). ERA-Interim is one of the most widely used reanalysis products (Tastula et al. 2013). ERA-5 is the latest climate reanalysis produced by ECMWF (Gossart et al. 2019).

ERA-5 improves upon ERA-Interim in various aspects. One of the major improvements of ERA-5 is the much higher spatial and temporal resolution (Hoffmann et al. 2019). ERA-5 data uses a spatial resolution of 37 km (62km for the Ensemble of Data Assimilations) in latitude and longitude, with atmospheric parameters on 137 levels in the vertical from the surface up to 0.01 hPa (Hersbach et al. 2020). The spatial resolution of the ERA-Interim is 79 km on 60 levels, covering the atmosphere from the surface up to 0.1 hPa (Berrisford et al. 2011). ERA-5 provides hourly data, compared to 6-hourly for ERA-Interim, on over 240 atmospheric, terrestrial, and oceanic climate variables together with estimates of uncertainty, covering the time period from January 1950 to present. Moreover, ERA-5 assimilation system uses the current version of the Integrated Forecast System (IFS Cycle 41r2), improving the modelling and data assimilation on satellite observations and ozone (Balsamo et al. 2018; Gossart et al. 2019). In addition, improved snow scheme in ERA-5 can reduce the snow albedo bias, providing a more accurate simulation of snow processes than other products (Dutra et al. 2010).

According to the evaluation of near surface atmospheric variables in the two reanalysis products over Antarctica, ERA-5 performs better than previous reanalysis products on most of the variables we are interested in, especially temperature and snowfall (Gossart et al. 2019; Tastula et al. 2013).

Thus, to assess the target climate variables in from 1979 to 2017, we used reanalysis data from ERA-5, including surface (skin) temperature, 2 metre air temperature, wind at 10 metre height, the mean surface downward short-wave radiation flux and snowfall. The atmospheric

data at the location of MBS main core are used to present the climate at MBS ice core site. However, this location is within between grid points, so bilinear interpolation is used to estimate the value at MBS main core drill site by calculating the distance weighted average of the four nearest pixel values (Fig. 5).

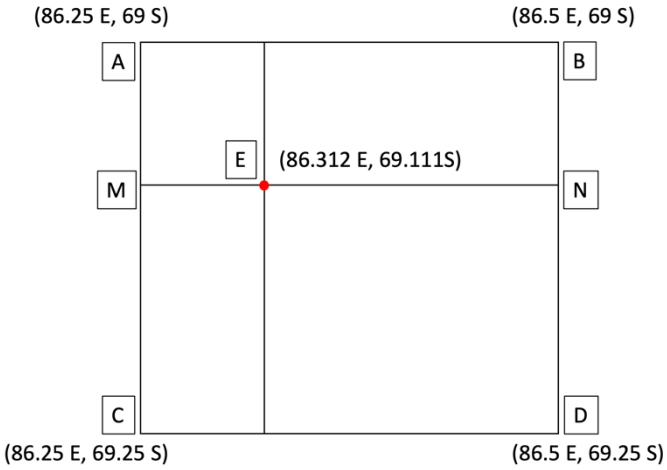

Figure 5 The location of Main core (E) and the four nearby pixels (A, B, C, D). First of all, weighted average of data at A and C is the data at M. Similarly, weighted average of data at B and D is the data at N. Data at E is the weighted average of data at M and N.

ERA-5 data used in this study were obtained from the Research Data Archive (https://rda.ucar.edu/).

Methods

1. Dating the ice core

The core chronology is established by direct counting of annual cycles in the Mount Brown South chemical and isotope records. The Mount Brown South chemical record contains seasonal cycles, which are used to date the ice core.

Support for this new dating scheme was provided by an increase in the sulphate signal during 1992–1994 from the volcanic eruption of Pinatubo, Philippines, (in 1991) and cross-matching of chemical signals (including the Pinatubo eruption) in a nearby core (MBS99) that spanned 19 years from 1979 to 1998 (Foster et al. 2006; Vance et al. 2016).

While there may be some uncertainty with the dating process before the Pinatubo eruption, it is unlikely to be more than one year. However, one year error would affect the findings presented in this paper.

2. Comparison with reanalysis data

In order to investigate the possibility that bubble-free layers represent local atmospheric signals, the times at which the atmospheric processes and bubble-free layers occur need to be compared. However, the variation of chemical composition in ice cores occurs only on year timescale. For more precise dating of bubble-free layers, as is required for analysis of the factors driving their formation, sub-annual dating of ice core becomes essential.

Reanalysis data can be used to get seasonal dating (Furukawa et al. 2017), but we need to first evaluate how well the reanalysis data represents the ice core data. So, first of all, we must investigate whether it can accurately represent a) the long-term mean accumulation; and b) the inter-annual variability seen in the ice core record, by investigating the correlation between reanalysis and ice core record of annual snowfall accumulation. If the correlation between the reanalysis snowfall and ice core accumulation is high and significant, this gives confidence when using monthly reanalysis accumulation totals to provide sub-annual dating. This allows estimation of the month when the bubble-free layers are generated. Furthermore, reanalysis-derived accumulation might also help with ice core dating in ambiguous years.

The annual accumulation at MBS ice core site are explored based on both ice core and reanalysis data. In order to obtain the annual accumulation from the ice cores, we independently dated the three ice cores using water isotopes and major ion chemistry. The annual snowfall accumulation for each year is determined by calculating the ice equivalent distance from one year horizon to the next. Then, the ice core annual accumulation is defined as the annual average accumulation of the three ice cores. Both the annual accumulation of the individual cores and the average accumulation of three core are compared with ERA-5 accumulation.

ERA-5 can not provide accumulation data directly. As the dominant processes which may influence the thickness of annual layers are wind and the accumulation rate of snow and the removal of such snow by wind redistribution, we use hourly ERA-5 snowfall and wind at 10 m height from ERA-5 to calculate annual accumulation at MBS. During periods of intense katabatic wind activity, large volumes of snowfall are typically resuspended, sublimated and/or transported into other sites (Li & Pomeroy 1997). Thus, ice accumulation can be approximated as total precipitation without the snow blown by the wind. The total precipitation is presented by total snowfall. As for wind-redistributed snow, it is essential to determine the wind speed when the snow particles become saltated. Then, when wind speed is higher than this threshold, the snowfall will not be counted as accumulation at MBS ice core site.

The minimum wind speed initiating or sustaining snow transport is estimated here through a sensitivity test. We test the snow transport wind speed threshold required to maximise the correlation coefficient between annual total ice core-derived and ERA-5 accumulation. Finally, ERA-5 derived accumulation is estimated as the total snowfall when the wind speed is less than the wind speed threshold.

With the annual accumulation of ice core data and ERA-5 data are calculated, the strength of the association between the two variables is then represented by calculating the correlation coefficient.

3. Dating the bubble free layers

Recent advances in analytical technologies have enabled ice core researchers to analyse polar ice cores at a high temporal resolution on annual to seasonal time scales (Hoshina et al. 2016; Iizuka, Hondoh & Fujii 2006; Steig et al. 2005). However, a more accurate monthly scale dating is required to achieve the aims outlined here. Since the annual variation of chemical composition in ice cores can only show the boundaries of each year, the relative monthly accumulation from ERA-5 helps determine the month of bubble-free layer formation. Measuring the distance between the year horizons and bubble free layers shows the accumulation during that time period (Fig.6). As mentioned before, ERA-5 snowfall and wind data can be used to estimate the amount of snow that have fallen at MBS since summer, until the total deposition is equal to that of the total annual accumulation. Then, we can get not only the year but also estimate the month when bubble free layers formed. However, due to a larger number of assumptions (namely that ERA-5 accurately represents accumulation), the confidence about monthly dating should be lower than annual dating.

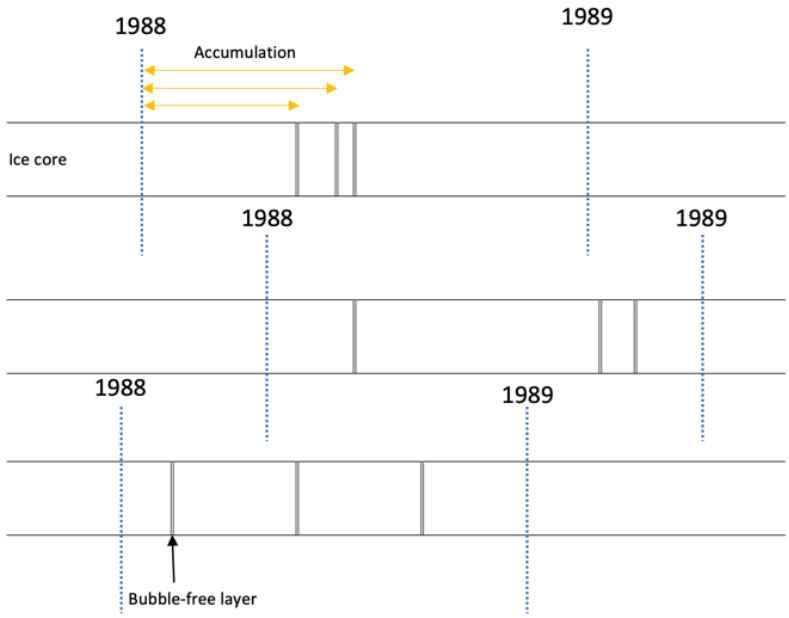

Figure 6 Schematic of estimating the seasonal date of bubble free layers: The yellow arrows present the accumulation from 1988 summer to the time when each bubble free layers formed. The calculated snowfall accumulation from the ice cores will be compared to the estimated accumulation at the site from ERA-5 precipitation for the grid cell that contains MBS to determine the within-year date of the bubble free layers.

The total number of bubble free layers across all three cores will be the primary metric used in subsequent analyses. However, because crusts that are present at the same time in two or three ice cores are more likely to be representative of large-scale atmospheric process, we also pay more attention to those layers that are common across the two or three ice cores (2+ common bubble free layer). Layer commonality was determined by manual visual inspection, noting which lines occurred in similar months.

4. Atmospheric process analyses

In addition to using ERA-5 to estimate month of bubble free layers occurrence, we also use it to investigate the potential atmospheric drivers of bubble free layers in the MBS ice cores. We use ERA-5 to represent the processes of near surface air temperature inversion, wind scour, accumulation hiatus, radiation flux and high subsurface temperature gradient. These atmospheric conditions are detailed below. We not only study the effects of individual weather processes, but also the effects of multiple events occurring together.

Near surface air temperature inversion

Near surface air temperature inversion can create "crusts" through enhance firn metamorphism, which could be the mechanism producing bubble free layers in the MBS ice core. Temperature inversion is the phenomenon in which the atmospheric temperature increase with altitude. This is opposite to the normal lapse rate, whereby air temperature decreases with altitude. Over the Antarctic plateau, a high-pressure system brings low humidity, low wind and clear sky. The strong heat loss from the surface via radiation cools the lower levels of the atmosphere, resulting in the formation of temperature inversion (Mayfield & Fochesatto 2013).

The temperature profile is widely used to detect the occurrence of temperature inversion (Fegyveresi et al. 2018; Hudson & Brandt 2005). In this project, ERA-5 data is used to investigate if there is a tendency for the air to be colder at surface than at 2 m above ground during the time of bubble free layer formation. If the skin temperature is lower than the 2 metre temperature, we can expect that a temperature inversion happened during that time (Hudson & Brandt 2005).

Strength and duration are the main parameters to characterise a temperature inversion event. In this paper, strength is defined as the temperature difference between the surface and 2m above ground:

$$IS = T_{skin} - T_{2m}$$

Where IS is temperature inversion strength, T_{skin} is skin temperature (K), T_{2m} is the air temperature at 2m height (K).

Since bubble free layers appear only 0-7 times a year, we need to detect the inversion events with unusually high average strength and long duration. For this purpose, in the following sections the temperature inversion strength is averaged every 6h and defined as temperature inversion conditions (TIC). Histogram of the TIC is informative about the TIC threshold of strong temperature inversion. The TIC threshold is calculated by:

$$TICThreshold = \overline{TIC} + 4\sigma$$

Where $\overline{TIC}$ is the average value of TIC, σ is standard deviation. A threshold of 4 sigma was found to give probability of exceeding the threshold of about 0.15% in a 6 hours period with the TIC threshold estimated as 4.79 K/6 hours.

Strong temperature inversion events are predicted under the condition that TIC > 4.79 K/6 hours. Annual total distribution, monthly distribution and seasonality of those events will be shown in subsequent analyses.

Wind scour

Wind scour occurs where strong katabatic winds persistently polish at the ice surface (Fisher et al. 1983). On relatively steep slopes, wind moves down. Its velocity increases and exceeds the critical value at which it can remove surface snow and expose the ice below. If the strong wind blows persistently in a single direction, the upper ice layer will be polished and the metamorphism would be enhanced by wind-driven air movement due to ventilation, favouring “crusts” at snow surface (Das et al. 2013). Then, our hypothesis is that this “crust” ice may be the precursors of the bubble free layers. Thus, we apply the mean wind speed and wind persistence thresholds to detect wind scour events.

As mentioned before, since only 0-7 bubble free layers formed in a year, we select times with high speed and high persistence. First of all, the hourly wind speed is calculated by:

$$S = \sqrt{U^2 + V^2}$$

where U is the zonal wind component at 10 m height, V is the meridional wind component at 10 m height. As the wind persistence is a measure of the mean wind speed duration over a given period of time, in this study, we chose 6 h as the timescale of required wind persistence. 6 h is long enough to calculate a reasonable value and short enough to preserve diurnal variation. Then, the wind speed is averaged every 6 h and defined as mean wind speed (MWS). As with TIC, from the histogram of MWS, the mean wind speed threshold (MWST) is estimated as 18.89 m s^{-1}. The probability of a wind with MWS > MWST is about 0.15 %.

Secondly, in order to find wind blowing persistently in a single direction, we define P, a wind persistence metric (Fraser et al. 2016):

$$P = \frac{\sqrt{u^2 + v^2}}{s}$$

where u is the mean zonal wind component in 6 h, v is the mean meridional wind component in 6 h and s is the mean wind speed in 6 h. Wind persistence metric is a number between 0 to 1. The higher the value of the wind persistence metric, the higher the wind persistence. For this reason, we take wind persistence threshold (WPT) as 0.98.

Finally, wind scour is predicted under the condition that both MWS ≥ 18.89 m $s^{-}1$ and P > 0.98 are simultaneously satisfied. Annual distribution, monthly distribution and seasonality of those events will be generated in subsequent analysis.

Accumulation hiatus

Accumulation hiatus is defined as a set period of time with little to no snow accumulation (Courville et al. 2007). Without the cover of new surface snow, the firn layer will be progressively polished by the katabatic winds and becomes glaze surface. Surface albedo will also lower, allowing high absorption of heat during times of insolation. Thus, in order to find

the link between the glaze ice and bubble free layer in ice core, the main quantities of interest in accumulation hiatus events detection are daily accumulation (A) and hiatus duration (D).

In the comparison section, we have calculated the daily accumulation at Mount Brown South site. Based on local annual accumulation, the maximum daily accumulation cannot exceed 0.0002 m (water equivalent) when accumulation hiatus occurs. Simultaneously, only accumulations hiatus lasting more than eight days is considered as the cause of glazed ice surface. The threshold D (8 days) is determined by testing the number which can make the number of accumulation hiatus is on a level with the total number of bubble free layers in one core. Thus, accumulation hiatus of interest is determined by satisfying both A < 0.0002 m (water equivalent) and D > 8 days. Finally, annual distribution, monthly distribution and seasonality of those events will be generated in subsequent analyses.

Subsurface temperature gradient

Subsurface temperature gradient drives the firn metamorphism at snow surface (Bingham 2011). The surface "crusts" formed during metamorphism could be the precursors of the bubble free layers. In this work, subsurface temperature gradient is defined as a temperature increase with depth in the upper few centimetres of snow (red line, Fig. 7).

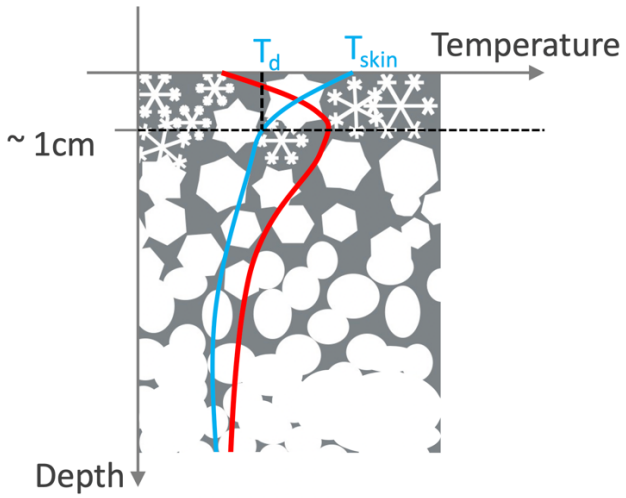

Figure 7 Snow temperature profiles. The red line presents the temperature gradient at the upper 1 cm snow. The blue line presents the negative temperature gradient below snow surface. T_d is the temperature of blue line at about 1 cm depth. T_{skin} is the temperature of blue line at snow surface. When a negative temperature gradient occurs, the temperature decreases with depth and $T_{skin} > T_d$.

In this study, the sign and strength of subsurface temperature gradient are indicated by the temperature difference between snow surface and subsurface temperature in the top few centimetres (TD):

$$TD = T_d - T_{skin}$$

Where T_d is the temperature at few centimetres depth, T_{skin} is the surface temperature.

As ERA-5 does not provide firn temperature data, the subsurface temperature in the top few centimetres can not be obtain directly from ERA-5. According to previous studies, the temperature below snow surface in the upper few centimetres is related to mean surface temperature over one to a few hours (Cuffey & Paterson 2010). So, the subsurface snow temperature is approximated by the hourly mean surface temperature which is the ERA-5 T_{skin} in previous hour. Then, the TD is estimated by,

$$TD = T_{skin\ before} - T_{skin}$$

where $T_{skin\ before}$ is the skin temperature in 1 h ago, T_{skin} is the surface temperature (for now).

High temperature gradient, or thermal inversions, happened when the upper snow surface is colder than snow beneath, or $T_{skin} < T_d$. So, high subsurface temperature gradience is predicted under the condition that TD > 2.9 k.

Annual distribution, monthly distribution and seasonality of those events will be generated in subsequent analysis.

Results

1. Comparison with reanalysis data

ERA-5 annual accumulation at the ice core site was approximately estimated by total precipitation without the snow blown by the wind. When the wind speed was higher than the minimum wind speed required to remove snow, snowfall during that period would be removed. The best estimation of the minimum wind speed would lead to the strongest correlation between ice core and ERA-5 annual accumulation. Figure 8 shows the result of this sensitivity test. As the threshold wind speed for snow transport increases towards infinity, the correlation coefficients between ice core and reanalysis data reach a peak of 0.48 and then remained relatively stable. It is evident that as long as wind speed for the initiation of snow transport is any value > 18 m s^{-1}, the correlation between the ice core and ERA-5 data are all strongest, which means that when neglecting the impact of wind transport, the ERA-5 accumulation data is most consistent with the ice core accumulation records. Thus, in this study, the ERA-5 snowfall accumulation at the ice core site was approximately estimated by total snowfall and no saltation threshold was used.

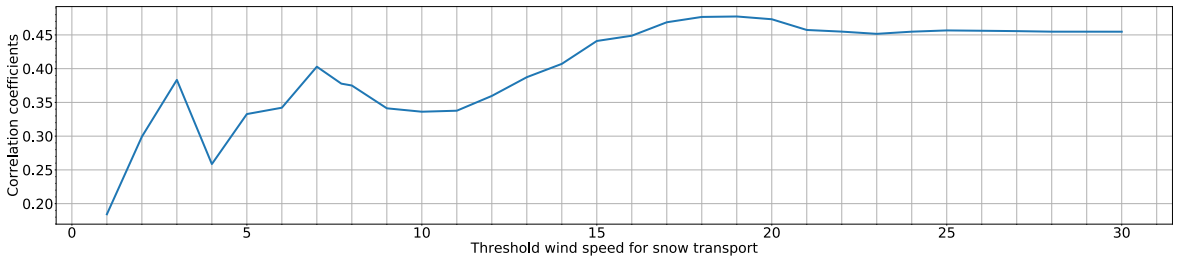

Figure 8 Sensitivity test of wind transport of snow 1979-2017. The threshold wind speed for snow transport (m s^{-1}) is the minimum wind speed initiating or sustaining saltation of snow. Correlation coefficient is the correlation coefficient between ice core and annual accumulation. Ice core accumulation is the annual average accumulation of three ice core in MBS site.

Since the ERA-5 accumulation data has been determined and we have calculated that total snowfall should be an accurate estimate of accumulation at the site, we compared it with ice core annual snowfall accumulation data. The timeseries of ice accumulation at the MBS site from 1979 to 2017 is shown in Fig. 9, for both ERA-5 and the ice core dataset. The result shows that except in several low accumulation years, the annual accumulation from those two different datasets is strongly correlated ($r = 0.455$, $p = 0.018$). The high reliability of the annual-layer dating permits estimation of the month of bubble-free layer formation in any given year.

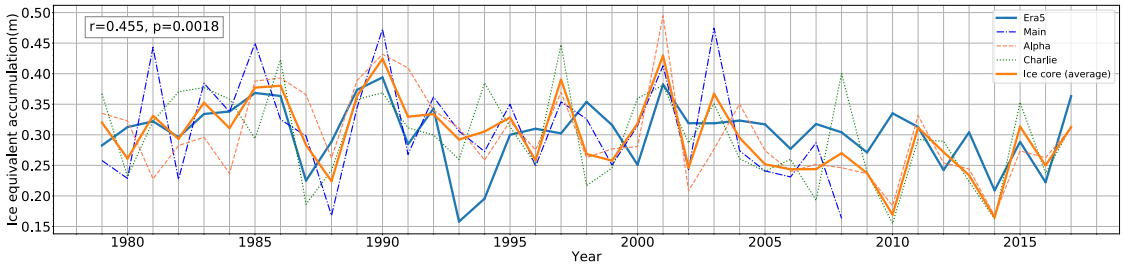

Figure 9 Comparison between ERA-5 and ice core annual accumulation.

2. Dating the bubble free layers

The boundaries of each year were identified by the annual variation of major chemistry ions and water isotopes in the ice cores. The relative monthly accumulation from ERA-5 for each year was used to identify the approximate relative position for each month of each year. We did this for each individual core which has been scanned with the ILCS, and we then used this within-year dating to identify the months when bubble-free layers formed (Fig. 10). All clear and identifiable bubble free layers identified from each core were marked, from 1979-2006. Layers since 2007 were not analysed, as the bubble free layers are more difficult to discern in the shallow ice. Each individual core has a slightly different accumulation for each year.

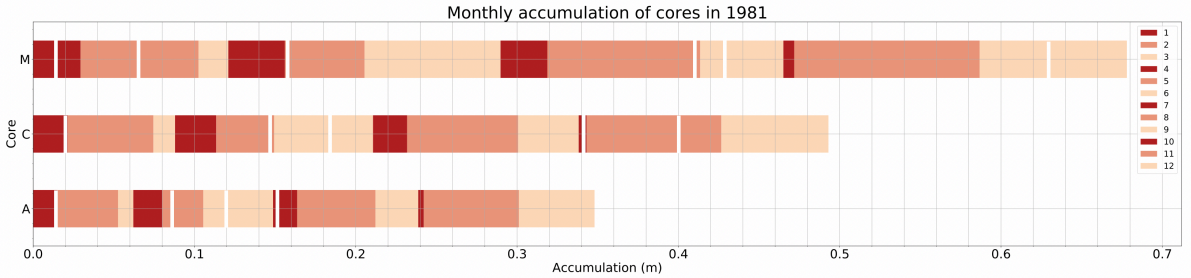

Figure 10. Monthly accumulation of three cores in 1981. A is Alpha core, C is Charlie core and M is the Main core. The length of bar present accumulation in each month (1: January; 2: February; . . . ; 12: December). The white line is the location of bubble free layer occurred in 1981.

Then, based on this high-precision dating, we explore the annual distribution, monthly distribution and seasonality of bubble free layers observed in the MBS cores.

A total of 308 bubble free layer (all bubble free layer) were identified in the top section of the three MBS cores. 200 bubble free layers are common across at least two cores at the same time (2+ common bubble free layer). A few were discontinuous across the core, and others appeared largely or completely continuous at the scale of the core. The number of bubble free layers per year common to two or more cores is significantly correlated to the number of bubble free layers for each year in all of the cores (r=0.685, P<0.001).

In Figure 11, the comparison between the number of bubble free layer (all) and the annual accumulation (ice core average) at MBS ice core site indicates that the number of bubble free layer may be not related to annual accumulation (r=0.327, P= 0.096).

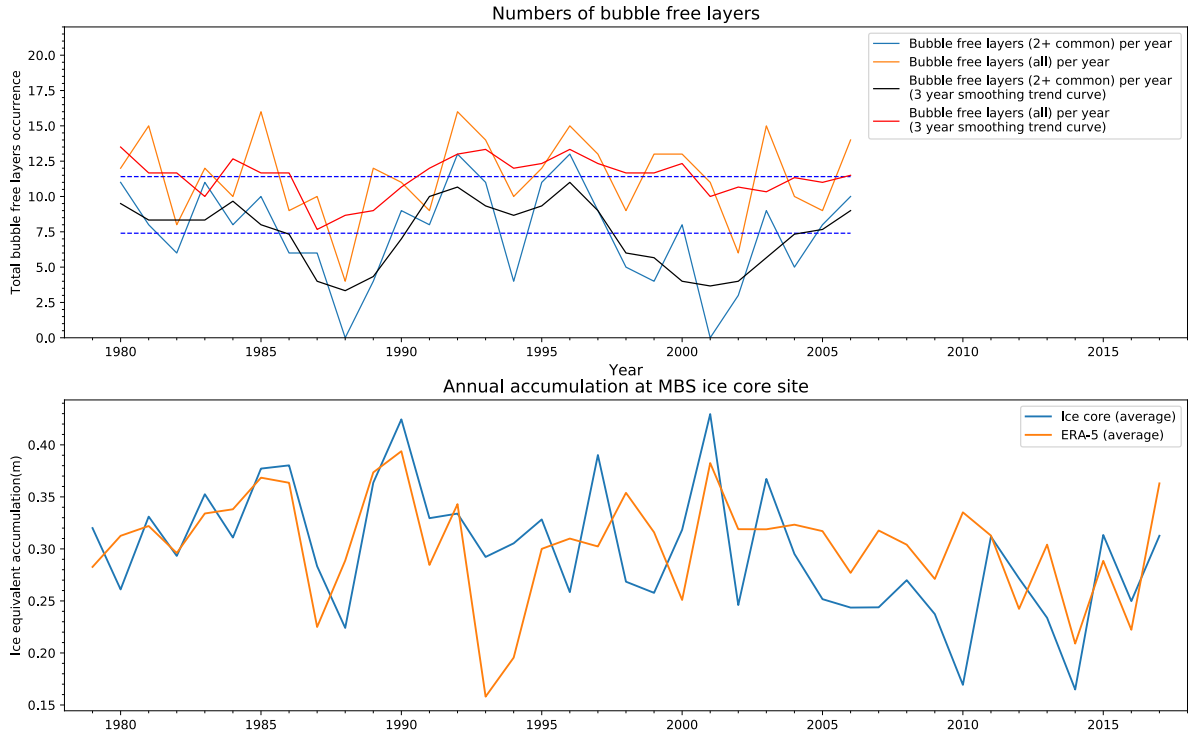

Figure 11.a) Occurrence of 2+ common bubble free layers (common across two and three cores) occurrence (layers year^{-1}), and total number of all bubble free layer occurrence (layer year^{-1}) in the three MBS cores that we studied in detail (0–~25 m depth). There are 308 bubble free layers in total. 200 of these were identified to be common to at least two cores. The average rate is about 11.4 bubble free layers per year and 7.4 per year respectively (dashed blue line). Data are shown with an added smoothing trend curve (3-year smooth). b) Annual accumulation at MBS ice site.

The number of bubble free layers per month common to two or more cores is significantly correlated to the number of bubble free layers for each month in all of the cores (r=0.969, P<0.001). At seasonal scale, the correlation between the number of bubble free layers

common to two or more cores and bubble free layer in all of the cores is still significant (r=0.999, P=0.001).

Bubble free layers occur year-round but are about 50 % more frequent in autumn (mostly from February to May) than in other seasons. This difference is larger in years with few layers (2+ common bubble free layers occurrence of each core < 5 layers year^{-1}) and smaller in years more layer (2+ common bubble free layers occurrence of each core > 4 layers year^{-1}).

3. Atmospheric process analyses

The results of comparisons of the bubble free layers and bubble free layers common in two or three ice cores with atmospheric processes are shown in Figure 12, Table 1 and Table 2. Most comparisons show an insignificant correlation. All atmospheric processes show insignificant with bubble free layers common in two or three ice cores.

Accumulation hiatus shows a significant correlation with bubble free layer formation at annual scale (r=0.381, P=0.038), but correlation in the seasonality and monthly variation is not significant. In the seasonal and monthly variation analyses, the correlation between two variables is -0.180 (p=0.41) and -0.079 (p=0.404) respectively, showing a non-significant relationship.

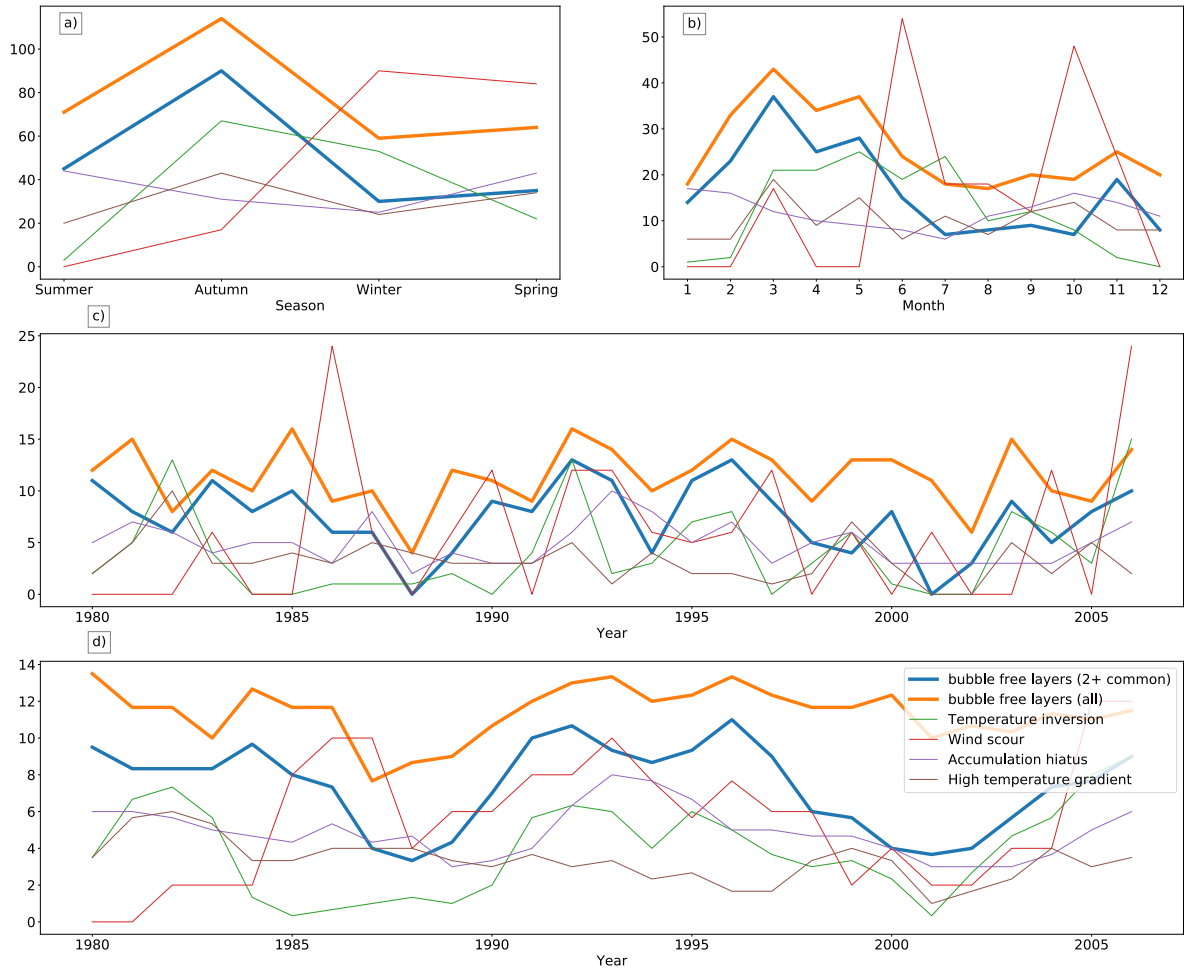

Figure 12 Atmospheric processes and bubble free layers analyses. a) the seasonality, b) the monthly climatology based on the assumption that each summer pick in the water isotopes and major ion chemistry is January, c) the annual variability, d) 3-year smoothed annual variability of atmospheric processes and bubble free layers. The analysis stops at 2006, because the bubble free layers formed after 2006 are not very clear and there are more ice core breaks after 2006.

Table 1 The correlation coefficient between 2+ common bubble free layers and each atmospheric process. The effective degrees of freedom (Neff) is calculated using lag 1 autocorrelation of the two timeseries. The significance is assessed based on two-tailed test at < 0.05.

Atmospheric processes	Seasonality (n=4)		Monthly variability (n=12)		Annual variability			Annual variability (3 point-smoothed)		
	r	P	r	P	r	P	N_{eff}	r	P	N_{eff}
Temperature inversion	0.534	0.233	0.367	0.120	0.366	0.066	25.5	0.570	0.14	7.6
Wind scour	-0.631	0.185	-0.284	0.185	0.169	0.390	26.9	0.211	0.558	9.7
Accumulation hiatus	-0.164	0.418	0.005	0.495	0.346	0.098	23.3	0.622	0.100	7.3
High temperature gradient	0.742	0.129	0.438	0.077	-0.017	0.931	26.8	0.08	0.826	9.8

Table 2 The correlation coefficient between total bubble free layers and each atmospheric process. *Red word indicates significant processes and correlations.*

Atmospheric processes	Seasonality (n=4)		Monthly variability (n=12)		Annual variability			Annual variability (3 point-smoothed)		
	r	P	r	P	r	P	N_{eff}	r	P	N_{eff}
Temperature inversion	0.557	0.222	0.435	0.079	0.322	0.083	28.3	0.368	0.195	12.1
Wind scour	-0.601	0.200	-0.272	0.196	0.204	0.318	24.8	-0.004	0.989	13.3
Accumulation hiatus	-0.180	0.410	-0.079	0.404	0.381	0.038	28.5	0.543	0.068	11.8
High temperature gradient	0.765	0.117	0.505	0.047	-0.002	0.994	27.2	-0.126	0.668	14

Discussion

1. Wind and snowfall effects on snow accumulation

As discussed earlier, an attempt was made to examine the transport of snow. The data shows that at the MBS ice core site:

(1) the amount of wind-driven snow transport exported is roughly equivalent to the amount imported.

(2) snowfall is the most significant factor which controls the amount of snow accumulation.

Physical understanding and data from previously published studies indicates that as long as the wind speed is high enough, snow transport will be initiated and sustained (Pomeroy 1991; Pomeroy & Male 1992). The MBS ice core site is in a dry snow zone with a relatively high annual accumulation and persistent katabatic winds. The ERA-5 10 m average wind speed at the MBS ice core site is 10.3 m s^{-1}, and the maximum speed can reach 29.4 m s^{-1}. Comparing it with the threshold of wind speeds for dry snow transport estimated by Li and Pomeroy (1997), from 4 to 11 m s^{-1} with an average of 7.7 m s^{-1}, we can know that, at MBS ice core site, the wind-driven snow transport happens most of the time. Thus, the insignificant wind effect on snow accumulation is not resulting from a lack of wind-driven snow transport. On the contrary, the high frequency of wind-driven snow transport leads to constantly change on surface snow mass. However, according to the results mentioned before, at the annual time scale, this wind-driven effect on snow accumulation is not significant.

A possible explanation is that the net wind-driven change in the amount of surface snow over a relatively long time scale can be approximated as 0. Although wind can move snow from one site and lead to accumulation being less than precipitation, it can also bring the snow from other places to fill up snow losses. Finally, the wind-driven snow loss and snow gain become roughly the same. Thus, wind-driven local snow transport can only be detected in a short time period. At monthly or annual scales, the net wind transport is insignificant. Correspondingly, the total accumulation at one site is only highly correlated with local snowfall.

2. Independent annual dating comparison with ERA-5

Accurate quantification of surface snow accumulation over Antarctica is a key constraint for estimates of the Antarctic mass balance, as well as climatic interpretations of ice-core records. From the comparison between ERA-5 average annual accumulation and the unadjusted average ice core annual accumulation, overall, the ERA-5 accumulation is found to be in agreement with unadjusted ice core accumulation ($r = 0.387$, $p = 0.07$). However, the result of ice core dating using the chemical and isotopic species indicated that there are two low accumulation years at MBS were probably over-estimated. ERA-5 accumulation confirmed this assumption. Thus, based on the assumption that there are two low accumulation years over 1979 to 2017 in MBS ice core, the dating was re-examined independently. Finally, the correlation between ERA-5 and ice core annual accumulation is improved ($r = 0.455$, $p = 0.0018$). This result indicates that:

(1) the close correlation between ERA-5 and ice core accumulation (especially around years with closely constrained dating) gives us high confidence in the ability of ERA-5 to represent annual accumulation.
(2) the annual accumulation estimated using ERA-5 can only be regarded as a reference to improve the identification of the within-year timing of the bubble-free layers, rather than an aid to dating.
(3) the dating errors detected using ERA-5 accumulation over 1979 to 2019, especially low accumulation years, will need to be considered when dating the rest of MBS ice core prior to the satellite era (full 1000 years before 1979).
(4) the high correlation between ERA-5 and the re-examined ice core annual accumulation shows that the re-examined MBS ice core layer counted dating from 1979 to 2017 is relatively accurate for the purposes of this study.
(5) the re-examined annual dating (informed by ERA-5) and the high correlation between ERA-5 and the re-examined core record on an annual basis give us this confidence for monthly dating of the bubble-free layers.

The annual dating is established by identifying the annual cycle in chemical and isotope records. However, in some places, the annual cycle is unclear or ambiguous. Under the assumption of similar annual layer thickness for each year, low accumulation years may not be correctly identified, leading to a “lost” year. The comparison with ERA-5 annual

accumulation suggests the most common dating error in the longer Mount Brown South record will likely be due to low accumulation years that are not detected.

From 1979-2017, the ice core dating significantly correlates to the ERA-5 data. However, focusing on accumulation in some individual years, the ERA-5 estimation does not always match well, especially in the ERA-5 low accumulation year, 1987 and 1993.

In 1987, the ERA-5 shows a low accumulation while a low accumulation year in the ice core record occurs in 1988, which is an apparent one year mismatch in this low-accumulation year. This could be explained by the accumulation differences in three core sites or the dating error in Main and Alpha core.

In 1993, the ERA-5 accumulation is only 0.16 m, which is much lower than ice core accumulation in the same year, and the difference between the two estimations remains large in the next few years. Based on the assumption that the ERA-5 data do not have significant error in 1993, the accumulation in 1993 could be a thin layer in ice core, which could be regard as a part of one year rather than an individual annual layer, leading to an incorrect assigning of the year boundary at 1993. Then, the actual end of 1994 could be mistakenly estimated as the end of 1993. Consequently, the loss of one year will lead to a one-year shift for the following years. If so, all of the dating after 1993 will contain errors. However, first of all, the annual accumulation from ERA-5 and ice core records become in significant agreement ($p = 0.479$, $r=0.022$) again in the period from 2000 to 2017. Secondly, the last year of ice core dating is 2017 which is consist with the drilling time. Both of the two points provide evidence that the one-year shift does not have a significant impact on ice core annual dating for all years after 1993.

Overall, the MBS ice core annual-layer dating has relatively high reliability, especially in 1979-1992 and 2001-2017. The annual ERA-5 accumulation is significantly in agreement with annual ice core data from 1979 to 2017. This result provides a possibility to further improve the annual dating and establish the monthly dating for Main core, Alpha core and Charlie core for the purposes of identifying the month that bubble-free layers occurred in.

In addition, the ERA-5 accumulation data also help subsequent dating for MBS ice core. Through the adjustment (from the ERA 5 analysis) of ice core dating from 1979 to 2017, low accumulation years in layer-counting dating of the full record might be missed. It means that, for the dating of the full 1000 years before 1979, if the number of years between two volcanic

horizons is less than expected, a “lost year" that cannot be observed through layer-counting is a possible explanation. For example, counting annual horizons between the Kuwae eruption in 1458 and the Tambora eruption in 1815. The dates of eruptions are from documentary evidence, so they are fixed. The major volcanic eruptions are recorded in ice core by peaks of sulphate concentration. From this study, if the number of annual layers in between the two volcanic horizons is too few, some years are probably missed due to them being low accumulation. Especially when there are two low accumulation years together, like 1993 and 1994, they might be counted as one year and a year would be lost. Thus, "lost years" due to low annual accumulation will also need to be considered when dating the rest of MBS ice core.

3. Monthly dating from using ERA-5

The reasonable agreement between ERA 5 and ice core dating means we can attempt to date within any given year the season or month that bubble-free layers occurred. Although the annual ice core accumulation is significantly in agreement with annual ERA-5 accumulation over 27 years, there is still disagreement between the annual accumulation from layer counting compared to ERA-5. The disagreement indicates that there are still likely to be significant errors in the monthly dating of the bubble-free layers. So, not all the bubble-free layers can be dated reliably.

4. Related atmospheric processes

This study examined the correlation coefficients for the occurrence of bubble free layers and atmospheric processes at seasonal, monthly and annual scales. As mentioned before, the annual dating from ice core analyses is more reliable than the ERA-5 monthly dating, so the conclusion based on annual scale should be more reliable than the result on monthly scale. The three-year smoothed annual data could help to reduce the impact from annual dating errors. Thus, the conclusion based on the annual, including the annual variability and the three-year smoothed annual variability for bubble free layer and the atmospheric processes, is more reliable in this study.

The data shows that, accumulation hiatus is highly correlated with the bubble free layers formation at annual scales (Table 2). Although the relation determined using smoothed data and the relation between accumulation hiatus and bubble free layers common in two and

three ice cores is statistical insignificant, their correlation is still pretty close to significant (Table 1, Table 2).

This result indicates that

(1) The bubble free layer is more likely to be related to local climate, which can be used as a proxy for past climate.

(2) The accumulation hiatus are the atmospheric processes which may generate the bubble free layer in MBS ice cores.

(3) The possible mechanism is that accumulation hiatus may enhance firn metamorphism.

Bubble free layer

The correlation between bubble free layers that are common in two and three ice cores with accumulation hiatus is close to significant. This result indicants that the bubble free layers in MBS ice core are more likely to be a climate signal, rather than simply the result of local surface reworking.

The occurrence of bubble free layers in MBS ice cores in each year from 1980 to 2006 suggest the possibility that bubble free layers could be used as a proxy of accumulation hiatus in the past. The possible bubble free layers favouring mechanism is that accumulation hiatus may enhance firn metamorphism which driving the formation of a thin ice crust at snow surface. As the snow accumulation, that crust is preserved through the bubbly ice.

Bubble free layer is the first proxy proposed for accumulation hiatus. Extreme snowfall events have been recently shown to constitute a high percentage of all surface accumulation across Antarctica, and likely to be the main factor determining the year-toyer variability in accumulation across much of the continent (Turner et al. 2019; Wille et al. 2019). The ability to detect the accumulation hiatus in ice core records would be a powerful tool to investigate past climate variability at the synoptic scale.

Accumulation hiatus

As mentioned before, the possible mechanisms favouring bubble free layers formation is that accumulation hiatus can enhance the firm metamorphism. Firn metamorphism can be enhanced by multiple mechanisms related to accumulation hiatuses. The first mechanism is a large diurnal temperature difference due to no clouds. Diurnal temperature difference during accumulation hiatus could be lager, because accumulation hiatus happened without clouds. Clouds can reduce the diurnal temperature difference through trapping outgoing longwave infrared radiative flux and reflecting shortwave solar radiative flux back to space. Without the effect of clouds, lager diurnal temperature difference can enhance the extent of temperature gradient–driven metamorphic growth.

Secondly, after several days without snowfall, the snow will be less fresh (lower albedo) so will absorb more shortwave radiation, which also lead to the increase of subsurface temperature gradient.

Thirdly, a long surface exposure time during accumulation hiatus could also enhanced vapour transport facilitates the metamorphosis of the near-surface firm layers. The lack of snow accumulation at the hiatus site resulted the firn being exposed to growth-forcing temperature gradients (Albert et al. 2004).

5. Not related atmospheric processes

The data shows that temperature inversion, wind scour and high subsurface temperature gradient are insignificant for the bubble free layers formation (Table 1, Table 2). This result indicates that temperature inversion, wind scour and subsurface temperature gradient may not be related to the formation of bubble free layers in MBS ice cores.

Subsurface temperature gradient

The temperature gradient is the main process driving firn metamorphism during accumulation hiatus and temperature inversion. However, the results show that it may not significant on bubble free layer formation. This indicates that the way used to detect temperature gradient could be not a proper way to represent the firn metamorphism. Lack of an automatic weather station at the Mount Brown South site means we can not get the observed subsurface temperature data to test this.

Wind scour

As mentioned before, wind is one of the processes which can enhance the firn metamorphism. However, the results indicate that the wind scour may not be related to bubble free layer formation in MBS ice cores. One possible explanation is that most of the wind rather than only the extremely strong wind can help generate bubble free layers.

Conclusion

In Antarctica, near surface snow is significantly impacted and altered by weather-related processes, which produce features buried and preserved in deep ice. This study of the MBS ice cores shows that:

- The net wind-driven change in the amount of surface snow over a relatively long time scale can be approximated as zero. The amount of wind-driven snow transport that's exported is roughly equivalent to the amount that's imported. Thus, snowfall is the most significant factor which controls the amount of snow accumulation at the MBS ice core site.

- The significant correlation between ERA-5 and ice core accumulation (especially around years with closely constrained dating) suggests a high confidence in the ability of ERA-5 to represent annual accumulation at the MBS ice core site. The annual accumulation estimated using ERA-5 can be consider as an approach to identifying low accumulation year and indicates that low accumulation years may result in "missed year" errors in ice core dating prior to the satellite era.

- The ERA-5 monthly accumulation can be considered as a reference of sub-annual dating for ice core. But, due to the potential error that exists in annual ice core dating, there are still likely to be significant errors in the dating in some months.

- This work shows a significant correlation between the occurrence of the accumulation hiatus and bubble free layers. The possible mechanisms favouring bubble free layers formation is that accumulation hiatus can enhance the firm metamorphism, driving the formation of thin crust at the snow surface. As the snow accumulated, this crust is preserved within ice containing bubbles.

- This work indicates that the occurrence of bubble free layers could be used as a proxy of accumulation hiatuses in the past. This is the first proxy proposed for accumulation hiatuses. The ability to detect the episodic nature of accumulation in ice core records would be a powerful tool to investigate past climate variability at the synoptic scale.

However, additional work would be required:

- In future studies, a locally placed automatic weather station with a thermistor string is needed to directly measure the temperature of the firn and determine the subsurface temperature gradient.

- This is a very early study in three new cores using an interim dating scale. Further analyses are planned for these ice cores, including cross-dating with Continuous Flow Analysis chemistry data. This is likely to improve the accuracy of the MBS ice core dating, which may increase the confidence of the result in this study.

References

Albert, M 2002, 'Effects of snow and firn ventilation on sublimation rates', *Annals of Glaciology*, vol. 35, pp. 52-56.

Albert, M, Shuman, C, Courville, Z, Bauer, R, Fahnestock, M & Scambos, T 2004, 'Extreme firn metamorphism: impact of decades of vapor transport on near-surface firn at a low-accumulation glazed site on the East Antarctic plateau', *Annals of Glaciology*, vol. 39, pp. 73-78.

Balsamo, G, Dutra, E, Albergel, C, Munier, S, Calvet, J-C, Munoz-Sabater, J & De Rosnay, P 2018, 'ERA-5 and ERA-Interim driven ISBA land surface model simulations: which one performs better?', *Hydrology and Earth System Sciences*, vol. 22, no. 6, pp. 3515 - 3532.

Bendel, V, Ueltzhöffer, KJ, Freitag, J, Kipfstuhl, S, Kuhs, WF, Garbe, CS & Faria, SH 2013, 'High-resolution variations in size, number and arrangement of air bubbles in the EPICA DML (Antarctica) ice core', *Journal of Glaciology*, vol. 59, no. 217, pp. 972-980.

Berrisford, P, Dee, DP, Poli, P, Brugge, R, Mark, F, Manuel, F, Kållberg, PW, Kobayashi, S, Uppala, S & Adrian, S 2011, *The ERA-Interim archive Version 2.0*, ECMWF, Shinfield Park, Reading, <https://www.ecmwf.int/node/8174>.

Bingham, RG 2011, 'Book Review: The Encyclopedia of Snow, Ice and Glaciers', *Journal of Glaciology*, vol. 57, pp. 1171-1172.

Costi, J, Arigony-Neto, J, Braun, M, Mavlyudov, B, Barrand, NE, da Silva, AB, Marques, WC & Simões, JC 2018, 'Estimating surface melt and runoff on the Antarctic Peninsula using ERA-Interim reanalysis data', *Antarctic Science*, vol. 30, no. 6, pp. 379-393.

Courville, ZR, Albert, MR, Fahnestock, MA, Cathles IV, LM & Shuman, CA 2007, 'Impacts of an accumulation hiatus on the physical properties of firn at a low-accumulation polar site', *Journal of Geophysical Research: Earth Surface*, vol. 112, no. F2.

Cuffey, K & Paterson, WSB 2010, *The Physics of Glaciers 4th Edition*, Academic Press.

Das, I, Bell, R, Scambos, T, Wolovick, M, Creyts, T, Studinger, M, Frearson, N, Nicolas, J, Lenaerts, J & Van den Broeke, M 2013, 'Influence of persistent wind scour on the surface mass balance of Antarctica', *Nature Geosci*, vol. 6, pp. 367-371.

Dutra, E, Balsamo, G, Viterbo, P, Miranda, PMA, Beljaars, A, Schär, C & Elder, K 2010, 'An Improved Snow Scheme for the ECMWF Land Surface Model: Description and Offline Validation', *Journal of Hydrometeorology*, vol. 11, no. 4, pp. 899-916.

Fegyveresi, JM, Alley, RB, Muto, A, Orsi, AJ & Spencer, MK 2018, 'Surface formation, preservation, and history of low-porosity crusts at the WAIS Divide site, West Antarctica', *The Cryosphere*, vol. 12, no. 1, pp. 325-341.

Fisher, DA, Koerner, RM, Paterson, WSB, Dansgaard, W, Gundestrup, N & Reeh, N 1983, 'Effect of wind scouring on climatic records from ice-core oxygen-isotope profiles', *Nature*, vol. 301, no. 5897, pp. 205-209.

Fitzpatrick, JJ, Voigt, DE, Fegyveresi, JM, Stevens, NT, Spencer, MK, Cole-Dai, J, Alley, RB, Jardine, GE, Cravens, ED, Wilen, LA, Fudge, TJ & McConnell, JR 2014, 'Physical properties of the WAIS Divide ice core', *Journal of Glaciology*, vol. 60, no. 224, pp. 1181-1198.

Foster, AFM, Curran, MAJ, Smith, BT, Van Ommen, TD & Morgan, VI 2006, 'Covariation of Sea ice and methanesulphonic acid in Wilhelm II Land, East Antarctica', *Annals of Glaciology*, vol. 44, pp. 429-432.

Fraser, AD, Nigro, MA, Ligtenberg, SRM, Legresy, B, Inoue, M, Cassano, JJ, Kuipers Munneke, P, Lenaerts, JTM, Young, NW, Treverrow, A, Van Den Broeke, M & Enomoto, H 2016, 'Drivers of ASCAT C band backscatter variability in the dry snow zone of Antarctica', *Journal of Glaciology*, vol. 62, no. 231, pp. 170-184.

Fraser, AD, Young, NW & Adams, N 2014, 'Comparison of Microwave Backscatter Anisotropy Parameterizations of the Antarctic Ice Sheet Using ASCAT', *IEEE Transactions on Geoscience and Remote Sensing*, vol. 52, no. 3, pp. 1583-1595.

Fujii, Y & Kusunoki, K 1982, 'The role of sublimation and condensation in the formation of ice sheet surface at Mizuho Station, Antarctica', *Journal of Geophysical Research: Oceans*, vol. 87, no. C6, pp. 4293-4300.

Furukawa, R, Uemura, R, Fujita, K, Sjolte, J, Yoshimura, K, Matoba, S & Iizuka, Y 2017, 'Seasonal-Scale Dating of a Shallow Ice Core From Greenland Using Oxygen Isotope Matching Between Data and Simulation', *Journal of Geophysical Research: Atmospheres*, vol. 122, no. 20, pp. 10,873-810,887.

Gossart, A, Helsen, S, Lenaerts, JTM, Broucke, SV, Lipzig, NPMv & Souverijns, N 2019, 'An Evaluation of Surface Climatology in State-of-the-Art Reanalyses over the Antarctic Ice Sheet', *Journal of Climate*, vol. 32, no. 20, pp. 6899-6915.

Hersbach, H, Bell, B, Berrisford, P, Hirahara, S, Horányi, A, Muñoz-Sabater, J, Nicolas, J, Peubey, C, Radu, R, Schepers, D, Simmons, A, Soci, C, Abdalla, S, Abellan, X, Balsamo, G, Bechtold, P, Biavati, G, Bidlot, J, Bonavita, M, De Chiara, G, Dahlgren, P, Dee, D, Diamantakis, M, Dragani, R, Flemming, J, Forbes, R, Fuentes, M, Geer, A, Haimberger, L, Healy, S, Hogan, RJ, Hólm, E, Janisková, M, Keeley, S, Laloyaux, P, Lopez, P, Lupu, C, Radnoti, G, de Rosnay, P, Rozum, I, Vamborg, F, Villaume, S & Thépaut, J-N 2020, 'The ERA5 global reanalysis', *Quarterly Journal of the Royal Meteorological Society*, vol. n/a, no. n/a.

Hersbach, H & Dee, D 2016, *ECMWF*, viewed 29 July 2019, <https://www.ecmwf.int/en/newsletter/147/news/era5-reanalysis-production>.

Hines, KM, Bromwich, DH & Marshall, GJ 2000, 'Artificial Surface Pressure Trends in the NCEP–NCAR Reanalysis over the Southern Ocean and Antarctica* ', *Journal of Climate*, vol. 13, no. 22, pp. 3940-3952.

Hoshina, Y, Fujita, K, Iizuka, Y & Motoyama, H 2016, 'Inconsistent relationships between major ions and water stable isotopes in Antarctic snow under different accumulation environments', *Polar Science*, vol. 10, no. 1, pp. 1-10.

Hudson, SR & Brandt, RE 2005, 'A Look at the Surface-Based Temperature Inversion on the Antarctic Plateau', *Journal of Climate*, vol. 18, no. 11, pp. 1673-1696.

Iizuka, Y, Hondoh, T & Fujii, Y 2006, 'Na2SO4 and MgSO4 salts during the Holocene period derived by high-resolution depth analysis of a Dome Fuji ice core', *Journal of Glaciology*, vol. 52, no. 176, pp. 58-64.

Jouzel, J 2001, 'Ice Core Records and Relevance for Future Climate Variations', in CU Hammer & LO Bengtsson (eds), *Geosphere-Biosphere Interactions and Climate*, Cambridge University Press, Cambridge, pp. 256-270, DOI DOI: 10.1017/CBO9780511529429.018, via Cambridge Core (Cambridge University Press).

Legrand, M, Angelis, M & Maupetit, F 1993, 'Field investigation of major and minor ions along Summit (Central Greenland) ice cores by ion chromatography', *Journal of Chromatography A - J CHROMATOGR A*, vol. 640, pp. 251-258.

Legrand, M & Delmas, RJ 1985, 'Spatial and Temporal Variations of Snow Chemistry in Terre Adélie (East Antarctica)', *Annals of Glaciology*, vol. 7, pp. 20-25.

Lenaerts, JTM, van den Broeke, MR, van de Berg, WJ, van Meijgaard, E & Kuipers Munneke, P 2012, 'A new, high-resolution surface mass balance map of Antarctica (1979–2010) based on regional atmospheric climate modeling', *Geophysical Research Letters*, vol. 39, no. 4.

Li, L & Pomeroy, J 1997, 'Estimates of Threshold Wind Speeds for Snow Transport Using Meteorological Data', *Journal of Applied Meteorology - J APPL METEOROL*, vol. 36, pp. 205-213.

Maksym, T & Markus, T 2008, 'Antarctic sea ice thickness and snow-to-ice conversion from atmospheric reanalysis and passive microwave snow depth', *Journal of Geophysical Research: Oceans*, vol. 113, no. C2.

Masson-Delmotte, V, Delmotte, M, Morgan, V, Etheridge, D, Van Ommen, T, Tartarin, S & Hoffmann, G 2003, 'Recent southern Indian Ocean climate variability inferred from a Law

Dome ice core: New insights for the interpretation of coastal Antarctic isotopic records', *Climate Dynamics*, vol. 21, pp. 153-166.

Mayfield, JA & Fochesatto, GJ 2013, 'The Layered Structure of the Winter Atmospheric Boundary Layer in the Interior of Alaska', *Journal of Applied Meteorology and Climatology*, vol. 52, no. 4, pp. 953-973.

Minikin, A, Wagenbach, D, Graf, W & Kipfstuhl, J 1994, 'Spatial and seasonal variations of the snow chemistry at the central Filchner-Ronne Ice Shelf, Antarctica', *Annals of Glaciology*, vol. 20, pp. 283-290.

Orsi, AJ, Kawamura, K, Fegyveresi, JM, Headly, MA, Alley, RB & Severinghaus, JP 2015, 'Differentiating bubble-free layers from melt layers in ice cores using noble gases', *Journal of Glaciology*, vol. 61, no. 227, pp. 585-594.

Oza, S, Singh, R, Vyas, N & Sarkar, A 2011, 'Study of inter-annual variations in surface melting over Amery Ice Shelf, East Antarctica, using space-borne scatterometer data', *Journal of Earth System Science*, vol. 120, pp. 329-336.

Palmer, A, Van Ommen, T, Curran, M & Morgan, V 2001, 'Ice-core evidence for small solar-source of atmospheric nitrate', *Geophysical Research Letters*, vol. 28, pp. 1953-1956.

Pomeroy, JW 1991, 'Transport and sublimation of snow in wind-scoured alpine terrain', in.

Pomeroy, JW & Male, DH 1992, 'Steady-state suspension of snow', *Journal of Hydrology*, vol. 136, no. 1, pp. 275-301.

Porter, SE & Mosley-Thompson, E 2014, 'Exploring seasonal accumulation bias in a west central Greenland ice core with observed and reanalyzed data', *Journal of Glaciology*, vol. 60, no. 224, pp. 1065-1074.

Shoji, H & Langway, CC 1982, 'Air hydrate inclusions in fresh ice core', *Nature*, vol. 298, no. 5874, pp. 548-550.

Steig, EJ, Mayewski, PA, Dixon, DA, Kaspari, SD, Frey, MM, Schneider, DP, Arcone, SA, Hamilton, GS, Blue Spikes, V, Mary Albert, u, Meese, D, Gow, AJ, Shuman, CA, White, JWC, Sneed, S, Flaherty, J & Wumkes, M 2005, 'High-resolution ice cores from US ITASE (West Antarctica): development and validation of chronologies and determination of precision and accuracy', *Annals of Glaciology*, vol. 41, pp. 77-84.

Tastula, E-M, Vihma, T, Andreas, EL & Galperin, B 2013, 'Validation of the diurnal cycles in atmospheric reanalyses over Antarctic sea ice', *Journal of Geophysical Research: Atmospheres*, vol. 118, no. 10, pp. 4194-4204.

Trusel, LD, Frey, KE & Das, SB 2012, 'Antarctic surface melting dynamics: Enhanced perspectives from radar scatterometer data', *Journal of Geophysical Research: Earth Surface*, vol. 117, no. F2.

Turner, J, Phillips, T, Thamban, M, Rahaman, W, Marshall, GJ, Wille, JD, Favier, V, Winton, VHL, Thomas, E, Wang, Z, van den Broeke, M, Hosking, JS & Lachlan-Cope, T 2019, 'The Dominant Role of Extreme Precipitation Events in Antarctic Snowfall Variability', *Geophysical Research Letters*, vol. 46, no. 6, pp. 3502-3511.

Urraca, R, Huld, T, Gracia-Amillo, A, Martinez-de-Pison, FJ, Kaspar, F & Sanz-Garcia, A 2018, 'Evaluation of global horizontal irradiance estimates from ERA5 and COSMO-REA6 reanalyses using ground and satellite-based data', *Solar Energy*, vol. 164, pp. 339-354.

van Ommen, TD & Morgan, V 1997, 'Calibrating the ice core paleothermometer using seasonality', *Journal of Geophysical Research: Atmospheres*, vol. 102, no. D8, pp. 9351-9357.

Vance, T, L. Roberts, J, D. Moy, A, A. J. Curran, M, Tozer, C, Gallant, A, Abram, N, Van Ommen, T, Young, D, Grima, C, Blankenship, D & Siegert, M 2016, 'Optimal site selection for a high resolution ice core record in East Antarctica', *Climate of the Past Discussions*, vol. 12, pp. 595–610.

Welch, KA, Mayewski, PA & Whitlow, SI 1993, 'Methanesulfonic acid in coastal Antarctic snow related to sea-ice extent', *Geophysical Research Letters*, vol. 20, no. 6, pp. 443-446.

Wille, J, Favier, V, Dufour, A, Gorodetskaya, I, Turner, J, Agosta, C & Codron, F 2019, 'Atmospheric River Climatology of Antarctica', *Geophysical Research Abstracts*, vol. 21, pp. 1-1.